Recent Electroweak Results from the Tevatron

Breese Quinn
University of Mississippi
On behalf of the CDF and DØ Collaborations

XXIXth Rencontres de Physique de La Vallée d'Aoste
La Thuile, Italy, March 5, 2015

Outline

Diboson Production

- $WW + jets$:
  - Differential cross section of massive dibosons

Precision Z, W Distribution Measurements

- ϕ^*:
  - Transverse Z distribution
- A:
  - W production and decay electron charge asymmetries
- θ_W:
  - Weak mixing angle from forward-backward Z asymmetry

WW+jets

CDF note 11098

Measurement of the W^+W^- Production Cross Section and Differential Cross Sections with Jets in $p\bar{p}$ Collisions at $\sqrt{s} = 1.96$ TeV

The CDF Collaboration
URL http://www-cdf.fnal.gov
(Dated: June 19, 2014)

CDF Public Note 11098

W^+W^- Production

- Produced through radiation from quarks

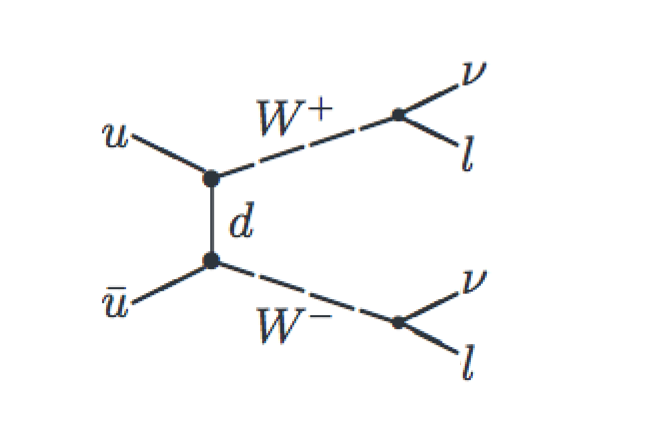

- multiple gauge boson coupling

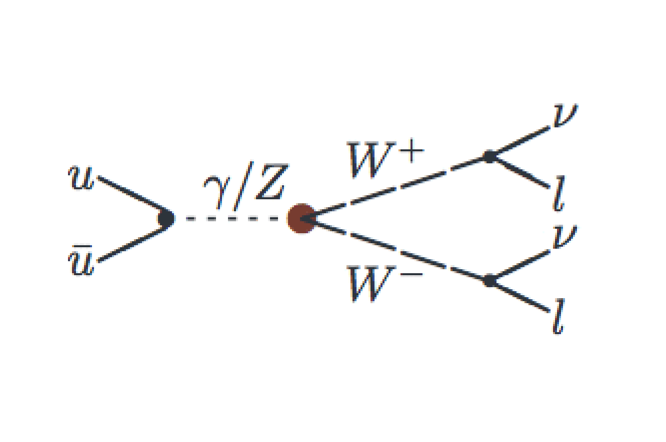

- Critical background for $H \rightarrow W^+W^-$
- Cross section measurement similar to HWW search
  - Extended to include events with 1 and 2 or more jets
  - 1 jet region subdivided by leading jet E_T

W^+W^-+jets Analysis Strategy

- **Select events with 2 charged leptons (e, μ), significant missing E_T**
- **Separate events into 5 analysis bins:**
  - 0 jets; 1 jet: ($15<E_T<25$ GeV),($25<E_T<45$ GeV),($E_T>45$ GeV); 2 or more jets
- **Train NeuroBayes neural net to separate *WW* from background**
- **Extract cross sections using a binned maximum likelihood fit to the *WW* and background neural net output templates**

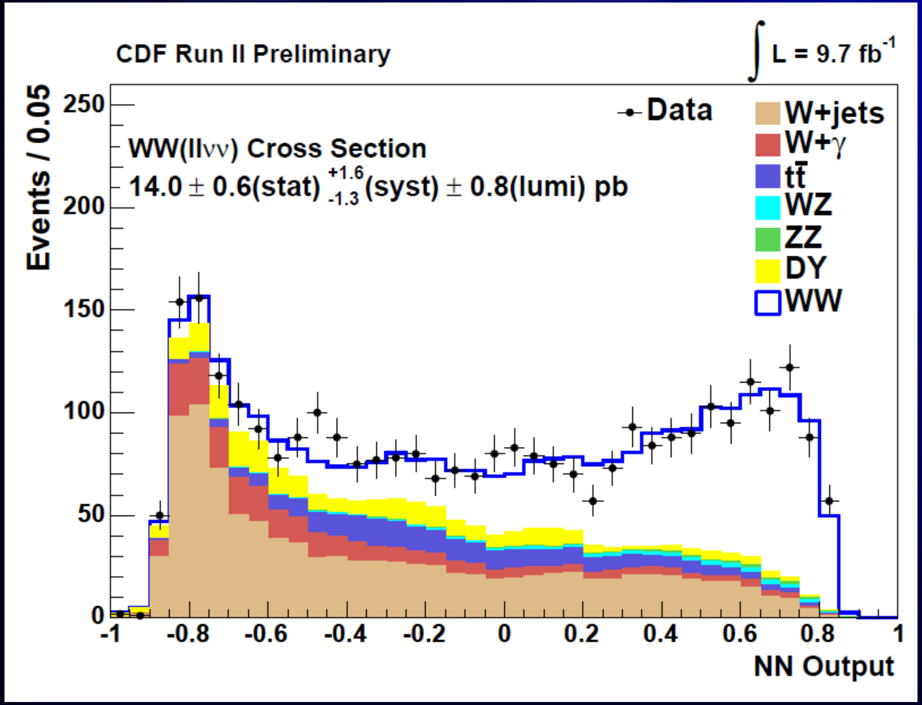

- **Neural net output combined distribution after fitting for all data**
- **Good modeling of neural net input variables is achieved for signal and background regions**

W^+W^- Results

- Results unfolded for bin migration and acceptance differences
- Uniformly higher than, but consistent with predictions

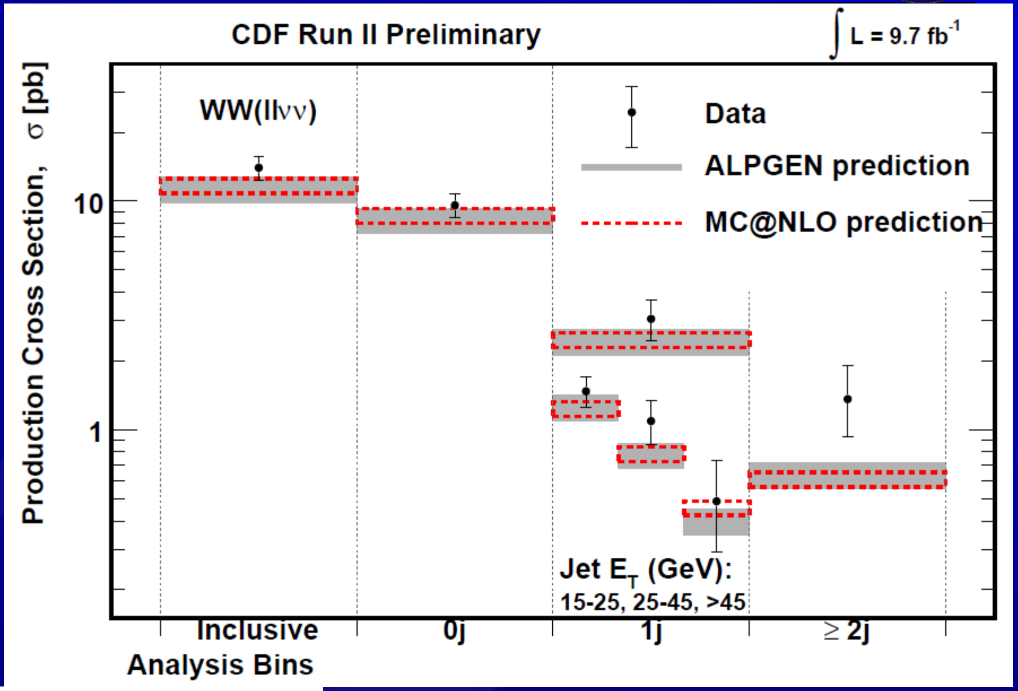

WW(llνν) Cross Section	CDF Run II Preliminary			$\int \mathcal{L} = 9.7$ fb^{-1}		
Jet Bin	σ(pb) Measured	Uncertainty(pb) Stat.	Syst.	Lumi.	σ(pb) Alpgen	MC@NLO
Inclusive	14.0	±0.6	$^{+1.6}_{-1.3}$	±0.8	11.3 ± 1.4	11.7 ± 0.9
0 Jets	9.6	±0.4	$^{+1.1}_{-0.9}$	±0.6	8.2 ± 1.0	8.6 ± 0.6
1 Jet Inclusive	3.05	±0.46	$^{+0.48}_{-0.32}$	±0.18	2.43 ± 0.31	2.47 ± 0.18
1 jet, $15 < E_T < 25$ GeV	1.47	±0.17	$^{+0.15}_{-0.11}$	±0.09	1.26 ± 0.16	1.18 ± 0.09
1 jet, $25 < E_T < 45$ GeV	1.09	±0.18	$^{+0.17}_{-0.12}$	±0.06	0.77 ± 0.10	0.79 ± 0.06
1 jet, $E_T > 45$ GeV	0.49	±0.15	$^{+0.20}_{-0.11}$	±0.03	0.40 ± 0.05	0.46 ± 0.03
2 or More jets	1.36	±0.30	$^{+0.46}_{-0.29}$	±0.08	0.64 ± 0.08	0.61 ± 0.05

- First differential σ in a massive diboson state
  - Very challenging at LHC due to $t\bar{t}$ background

Tevatron Precision EW: Why?

- **e.g. Need to understand proton structure better**
- **Kinematics coverage: For LHC, data fixed Q^2 spans wider x than the Tevatron**

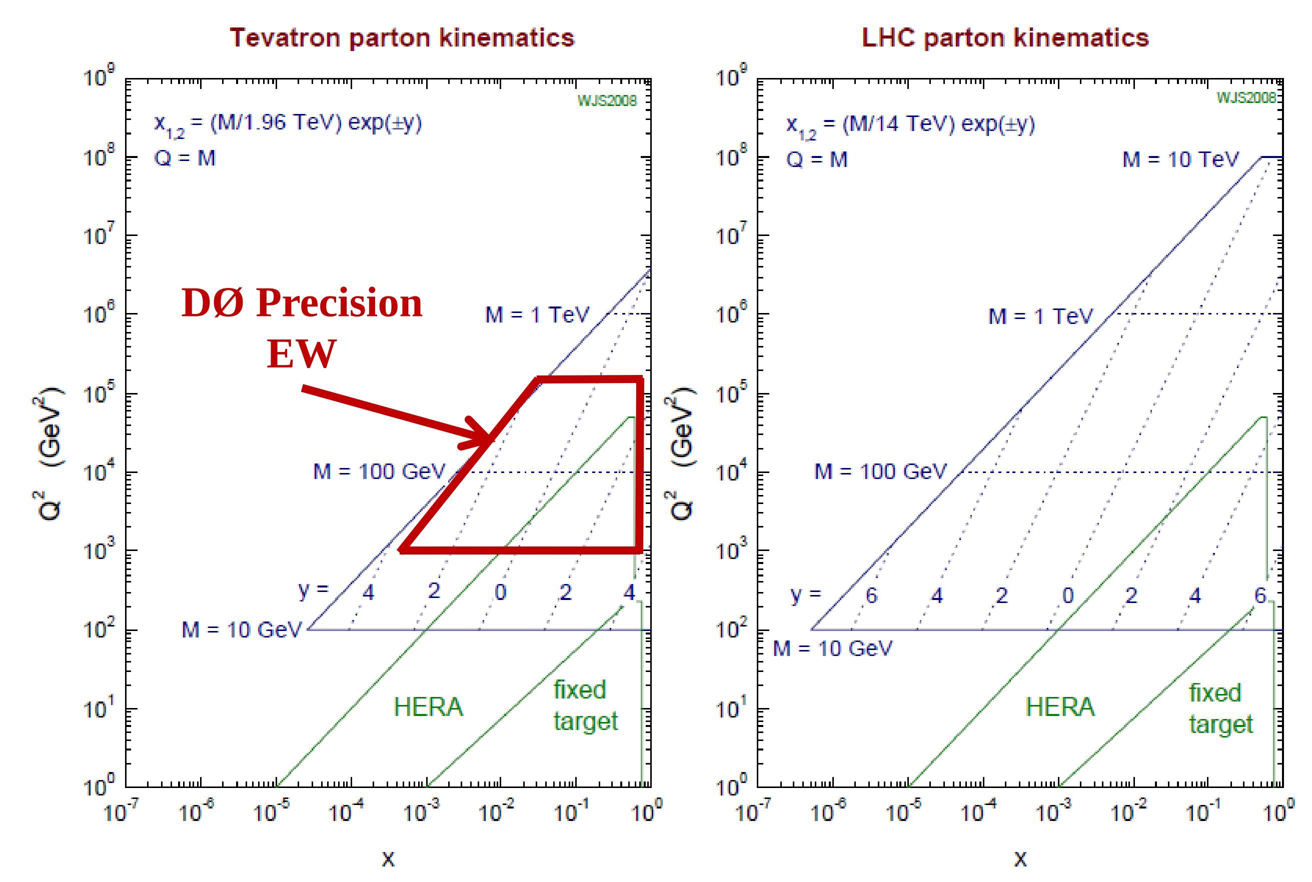

- Momentum transfer scale
  - $Q^2 \approx M_V^2$
- Parton momentum fraction
  - $x = \frac{M}{\sqrt{s}} e^{\pm y}$

  $0.002 < x < 1$
- Complementary to central and forward jet measurements at Tevatron, and other scattering expts.
  - Different systematics, couplings
  - Higher precision!

W Production at Tevatron/LHC

- Tevatron: dominated by valence quark production

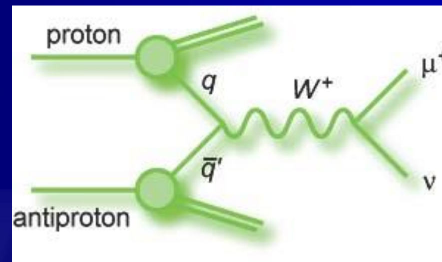

- LHC: dominated by sea quark and gluon production

- Tevatron measurements place stringent constraints on valence PDFs

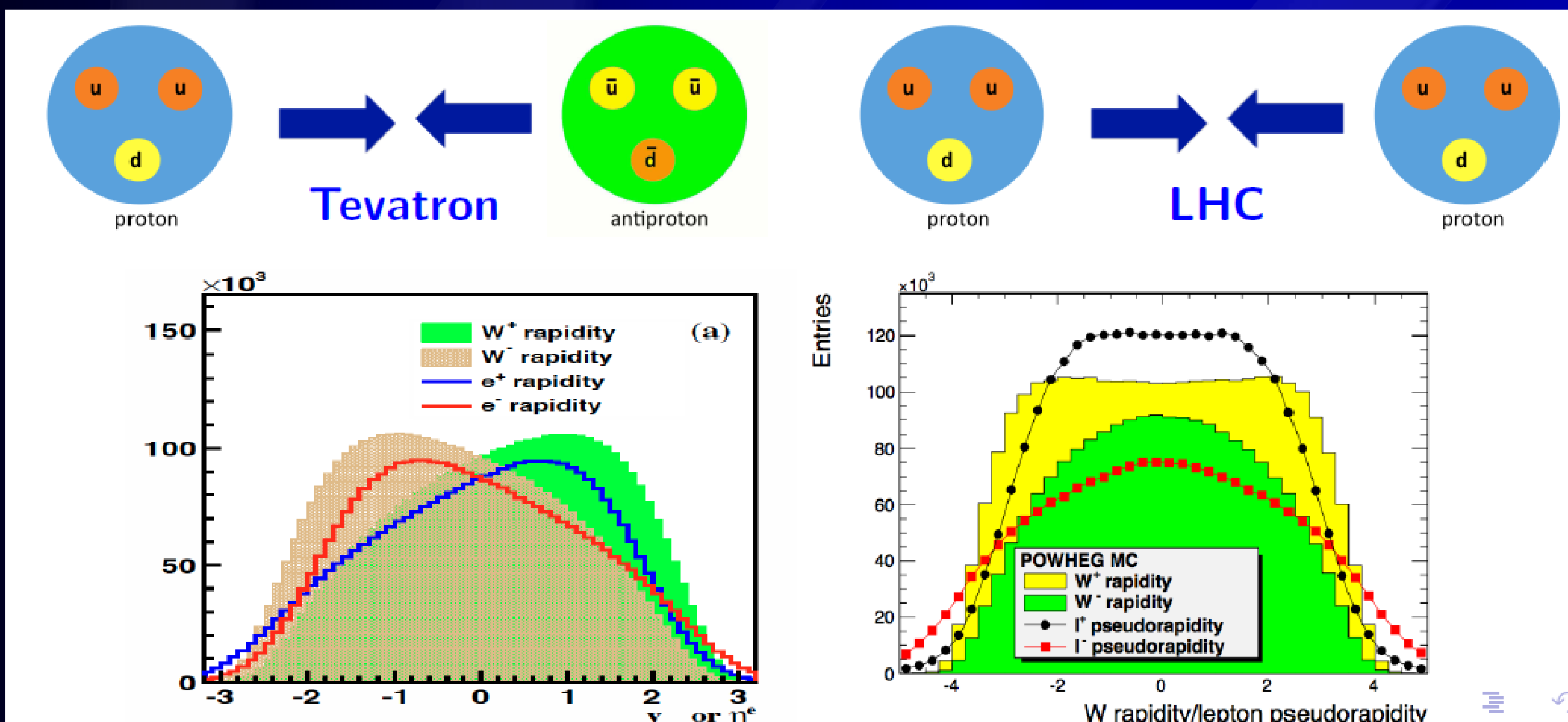

PDF Impacts: W Boson Mass

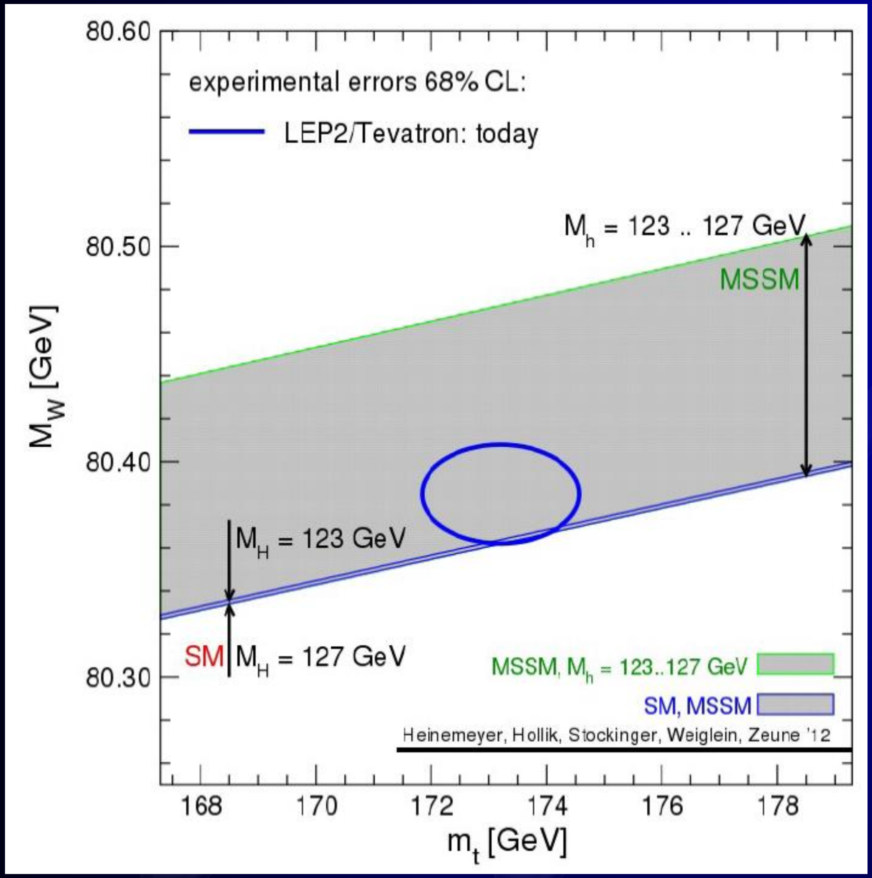

- GFitter collaboration arXiv:1407.3792

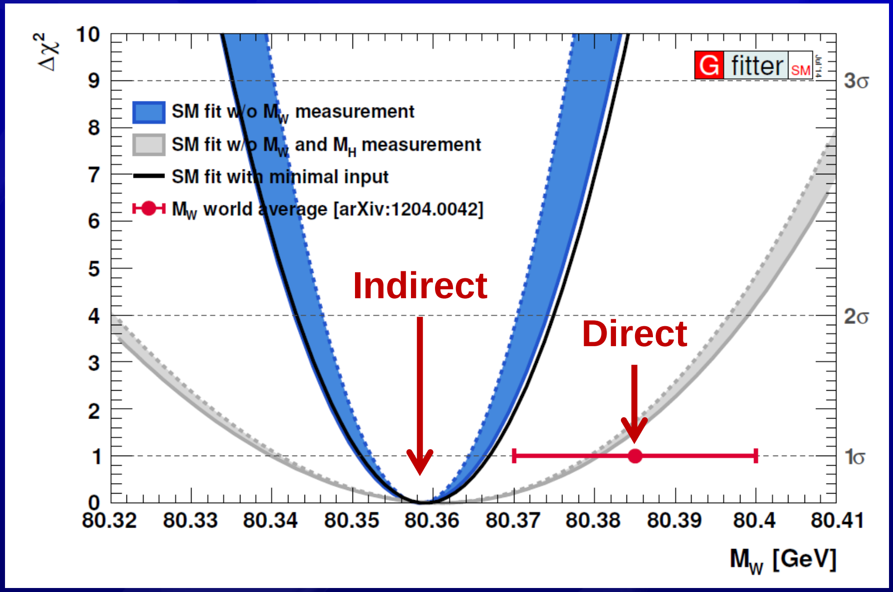

- PDF inputs to M_W measurement will contribute the largest uncertainty for the complete Tevatron data result unless PDF improvements are made.
- M_W direct measurement: (80.385 ± 0.015) GeV
- M_W indirect determination: (80.358 ± 0.008) GeV

ϕ^*

30 Oct 2014

Measurement of the ϕ^*_η distribution of muon pairs with masses between 30 and 500 GeV in 10.4 fb^{-1} of $p\bar{p}$ collisions

V.M. Abazov,[31] B. Abbott,[67] B.S. Acharya,[25] M. Adams,[46] T. Adams,[44] J.P. Agnew,[41] G.D. Alexeev,[31] G. Alkhazov,[35] A. Alton[a],[56] A. Askew,[44] S. Atkins,[54] K. Augsten,[7] C. Avila,[5] F. Badaud,[10] L. Bagby,[45] B. Baldin,[45] D.V. Bandurin,[73] S. Banerjee,[25] E. Barberis,[55] P. Baringer,[53] J.F. Bartlett,[45] U. Bassler,[15] V. Bazterra,[46] A. Bean,[53] M. Begalli,[2] L. Bellantoni,[45] S.B. Beri,[23] G. Bernardi,[14] R. Bernhard,[19] I. Bertram,[39] M. Besançon,[15] R. Beuselinck,[40] P.C. Bhat,[45] S. Bhatia,[58] V. Bhatnagar,[23] G. Blazey,[47] S. Blessing,[44] K. Bloom,[59] A. Boehnlein,[45] D. Boline,[64] E.E. Boos,[33] G. Borissov,[39] M. Borysova[l],[38] A. Brandt,[70] O. Brandt,[20] R. Brock,[57] A. Bross,[45] D. Brown,[14] X.B. Bu,[45] M. Buehler,[45] V. Buescher,[21] V. Bunichev,[33] S. Burdin[b],[39] C.P. Buszello,[37] E. Camacho-Pérez,[28] B.C.K. Casey,[45] H. Castilla-Valdez,[28] S. Caughron,[57] S. Chakrabarti,[64] K.M. Chan,[51] A. Chandra,[72] E. Chapon,[15] G. Chen,[53] S.W. Cho,[27] S. Choi,[27] B. Choudhary,[24] S. Cihangir,[45] D. Claes,[59] J. Clutter,[53] M. Cooke[k],[45] W.E. Cooper,[45] M. Corcoran,[72] F. Couderc,[15] M.-C. Cousinou,[12] D. Cutts,[69] A. Das,[42]

Accepted by Phys. Rev. D **arXiv:1410.8052**

03/02/15

ϕ^*: Definition

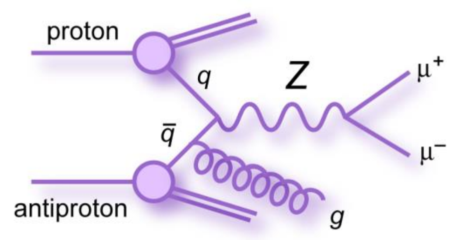

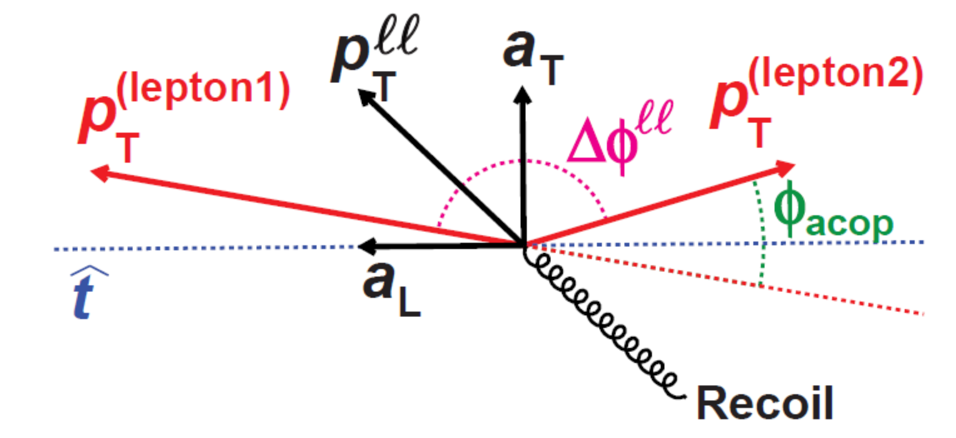

EPJ C71 1600(2011)

- $\boldsymbol{\phi^* = \tan(\phi_{acop}/2)\sin\theta^*}$
  - $\phi_{acop} = \pi - \Delta\phi^{ll}$
  - $\cos\theta^* = \tanh((\eta_- - \eta_+)/2)$ [Collins-Soper angle]
- **ϕ^* probes same physics as p_T^{ll}, $\phi^* \sim a_T/M_{ll}$**
- **ϕ^* less sensitive to detector resolution and efficiency**
  - Uses angles only (mrad precision with < 1% resolution vs. few % resolution on *p*, *E*)
- **First measured in peak region data by D0 (7.3 fb^{-1})**
  - PRL 106, 122001 (2011)
- **Data used to improve ResBos and make predictions for LHC**
  - ATLAS: PLB 720, 32(2013)
  - LHCb: JHEP 1302, 106(2013)

ϕ^*: Peak Region Results

- **ResBos:** Guzzi *et al.* *arXiv: 1309.1393*

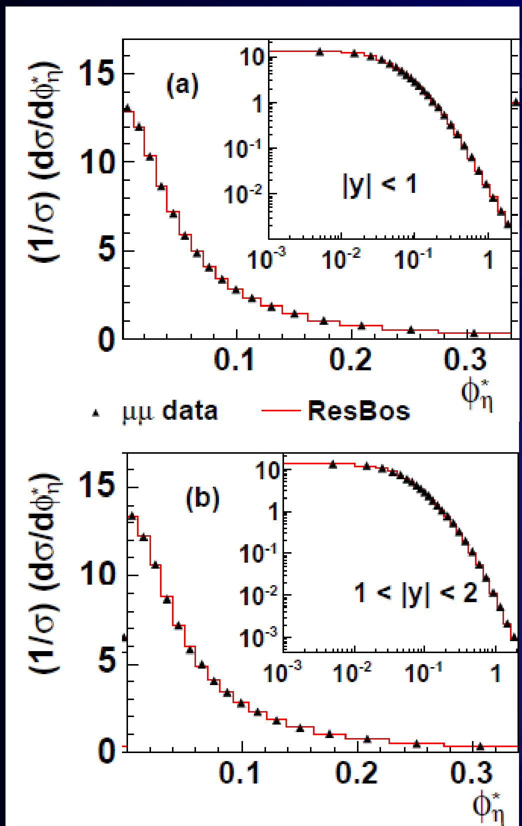

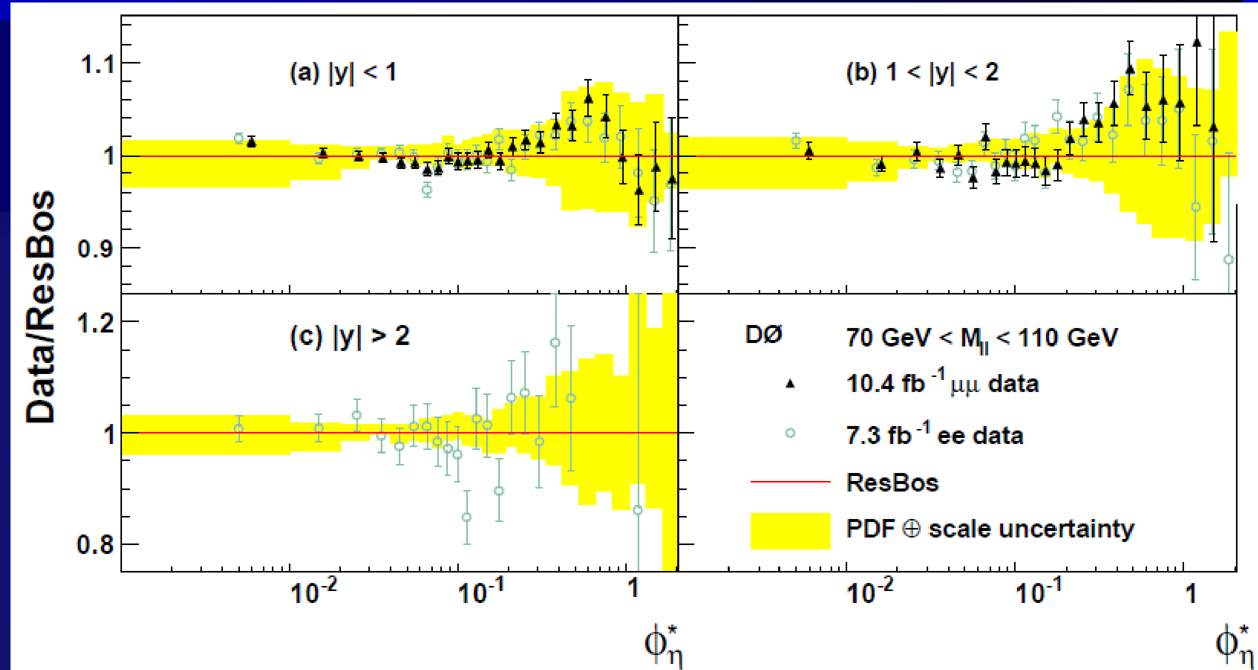

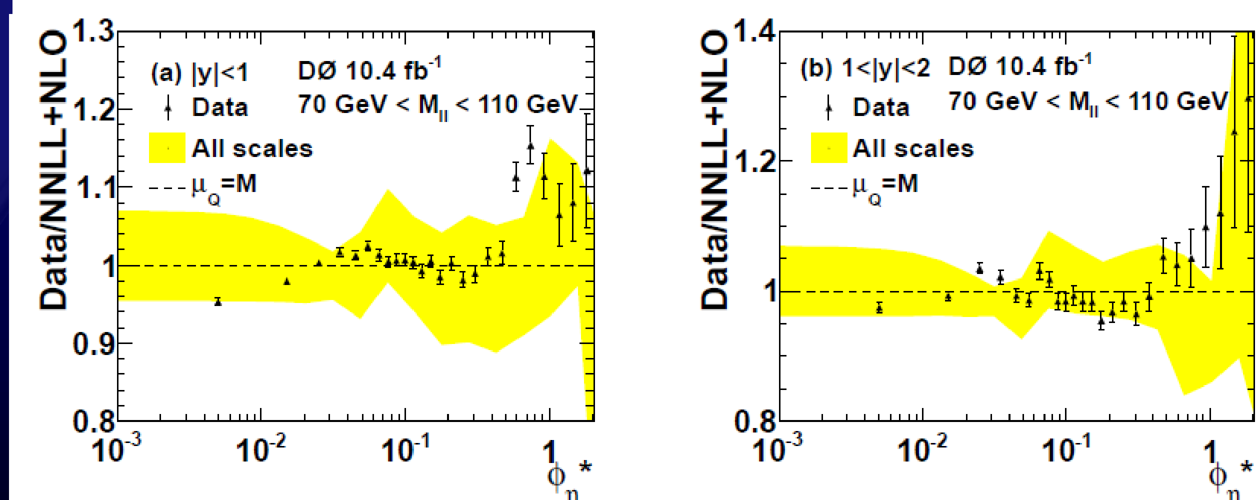

- **NNLL+NLO:** Banfi *et al.* *JHEP01 (2012) 044*

ϕ*: Peak Region Results

- **Ratio of $(1/\sigma)(d\sigma/d\phi^*)$ in rapidity bins**
  - The ratio $(1/\sigma)(d\sigma/d\phi^*)$ in the central rapidity region to that in the forward rapidity region can reduce the uncertainty band from QCD scales to the percent level due to cancellations. It suggests the possibility of a new variable that is less sensitive to theoretical uncertainty.

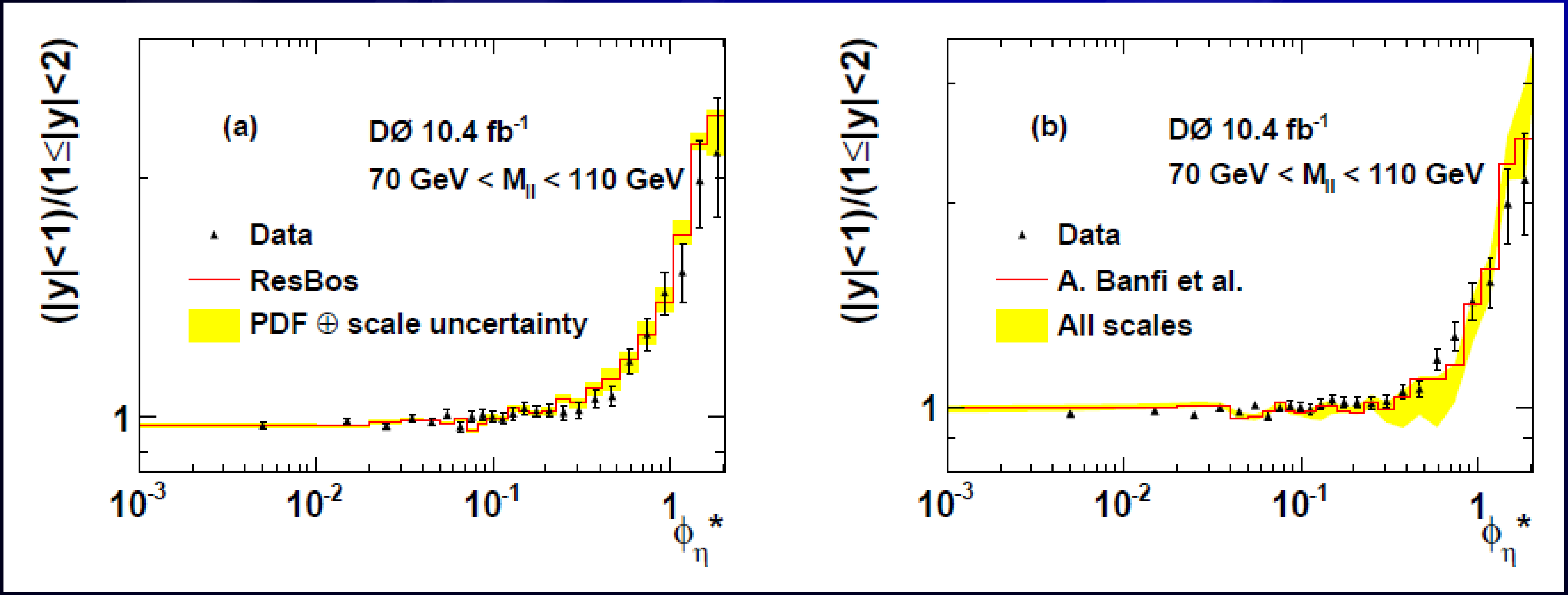

ϕ^*: Off-peak Region Results

- **First ever low mass measurement**
  - More sensitive to small-*x* effects
  - Statistically more powerful than peak forward rapidity region

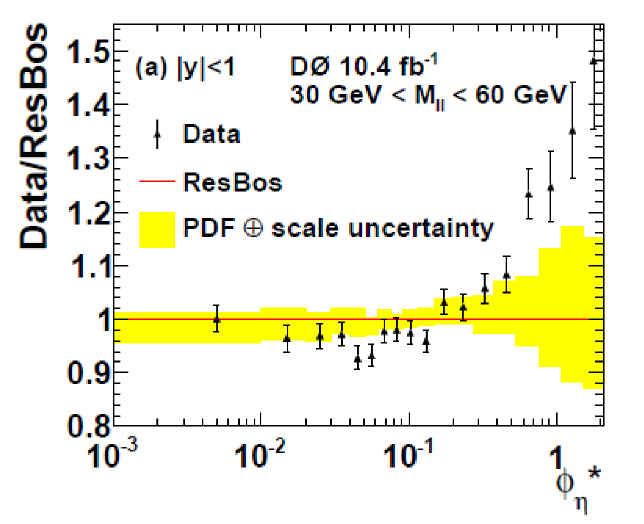

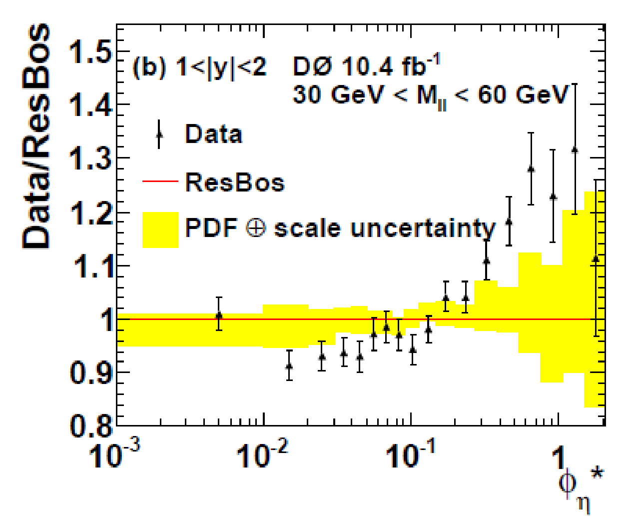

- **First ever high mass measurement**
  - For constraining QCD ISR in high mass final states, but limited statistics prevented detailed comparisons (see backup slides)

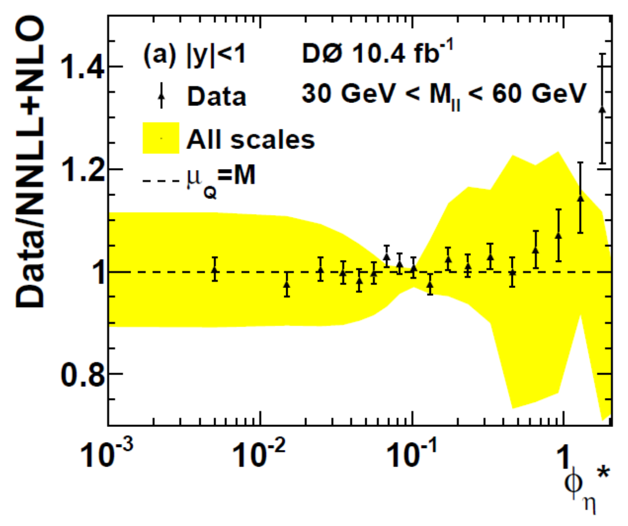

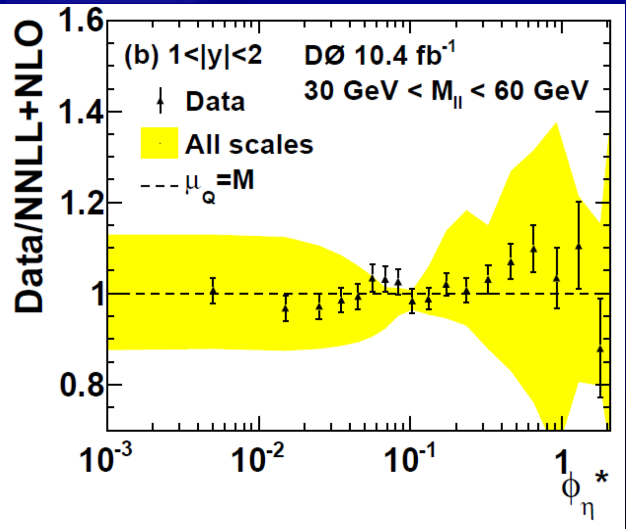

A

Measurement of the electron charge asymmetry in $p\bar{p} \rightarrow W + X \rightarrow e\nu + X$ decays in $p\bar{p}$ collisions at $\sqrt{s} = 1.96$ TeV

27 Jan 2015

V.M. Abazov,[31] B. Abbott,[67] B.S. Acharya,[25] M. Adams,[46] T. Adams,[44] J.P. Agnew,[41] G.D. Alexeev,[31] G. Alkhazov,[35] A. Alton[a],[56] A. Askew,[44] S. Atkins,[54] K. Augsten,[7] C. Avila,[5] F. Badaud,[10] L. Bagby,[45] B. Baldin,[45] D.V. Bandurin,[73] S. Banerjee,[25] E. Barberis,[55] P. Baringer,[53] J.F. Bartlett,[45] U. Bassler,[15] V. Bazterra,[46] A. Bean,[53] M. Begalli,[2] L. Bellantoni,[45] S.B. Beri,[23] G. Bernardi,[14] R. Bernhard,[19] I. Bertram,[39] M. Besançon,[15] R. Beuselinck,[40] P.C. Bhat,[45] S. Bhatia,[58] V. Bhatnagar,[23] G. Blazey,[47] S. Blessing,[44] K. Bloom,[59] A. Boehnlein,[45] D. Boline,[64] E.E. Boos,[33] G. Borissov,[39] M. Borysova[l],[38] A. Brandt,[70] O. Brandt,[20] R. Brock,[57] A. Bross,[45] D. Brown,[14] X.B. Bu,[45] M. Buehler,[45] V. Buescher,[21] V. Bunichev,[33] S. Burdin[b],[39] C.P. Buszello,[37] E. Camacho-Pérez,[28] B.C.K. Casey,[45] H. Castilla-Valdez,[28] S. Caughron,[57] S. Chakrabarti,[64] K.M. Chan,[51] A. Chandra,[72] E. Chapon,[15] G. Chen,[53] S.W. Cho,[27] S. Choi,[27] B. Choudhary,[24] S. Cihangir,[45] D. Claes,[59] J. Clutter,[53] M. Cooke[k],[45] W.E. Cooper,[45] M. Corcoran,[72] F. Couderc,[15] M.-C. Cousinou,[12] D. Cutts,[69] A. Das,[42] G. Davies,[40] S.J. de Jong,[29,30] E. De La Cruz-Burelo,[28] F. Déliot,[15] R. Demina,[63] D. Denisov,[45] S.P. Denisov,[34] S. Desai,[45] C. Deterre[c],[41] K. DeVaughan,[59] H.T. Diehl,[45] M. Diesburg,[45] P.F. Ding,[41] A. Dominguez,[59] A. Dubey,[24] L.V. Dudko,[33] A. Duperrin,[12] S. Dutt,[23] M. Eads,[47] D. Edmunds,[57] J. Ellison,[43] V.D. Elvira,[45] Y. Enari,[14] H. Evans,[49] V.N. Evdokimov,[34] A. Fauré,[15] L. Feng,[47] T. Ferbel,[63] F. Fiedler,[21] F. Filthaut,[29,30] W. Fisher,[57] H.E. Fisk,[45] M. Fortner,[47] H. Fox,[39] S. Fuess,[45] P.H. Garbincius,[45]

Phys. Rev. D 91, 032007 (2015) arXiv:1412.2862

02/18/15

A: Introduction

- W charge asymmetry is sensitive to Parton Distribution Functions (PDFs)
  - In $p\bar{p}$ colliders, u and $\bar{u}$ quarks have higher momentum than d and $\bar{d}$ quarks
  - $W^+(W^-)$ are preferentially produced in the $p(\bar{p})$ direction
- Provides a strong constraint on u and d PDFs
- The W asymmetry in the leading order parton model is

$$A(y_W) = \frac{\frac{d\sigma^+}{dy_W} - \frac{d\sigma^-}{dy_W}}{\frac{d\sigma^+}{dy_W} + \frac{d\sigma^-}{dy_W}} = \frac{u(x_p)\bar{d}(x_{\bar{p}}) - d(x_p)\bar{u}(x_{\bar{p}})}{u(x_p)\bar{d}(x_{\bar{p}}) + d(x_p)\bar{u}(x_{\bar{p}})}$$

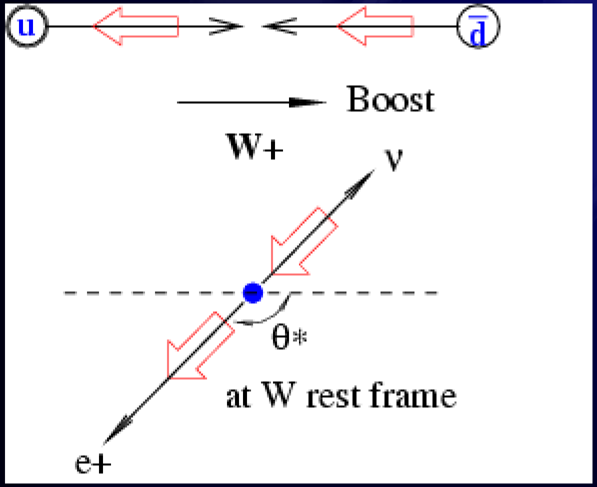

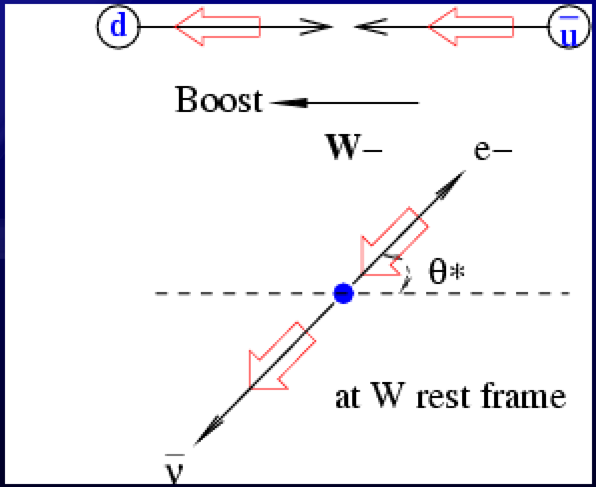

A: Introduction

- **The lepton asymmetry is a convolution of the *W* production asymmetry and the *V−A* decay: important to measure lepton and *W* asymmetry**
- **Lepton asymmetry:** More straightforward observable, easier to measure than *W*
- ***W* asymmetry:**
  - Advantage over lepton: Due to convolution, leptons at a specific pseudorapidity (η) originate from a wide range of *W* rapidities, and therefore from a wide range of parton *x* values, making these asymmetries less useful in determining PDFs.
  - Challenge: With unknown neutrino p_Z, difficult to determine the *W* rapidity

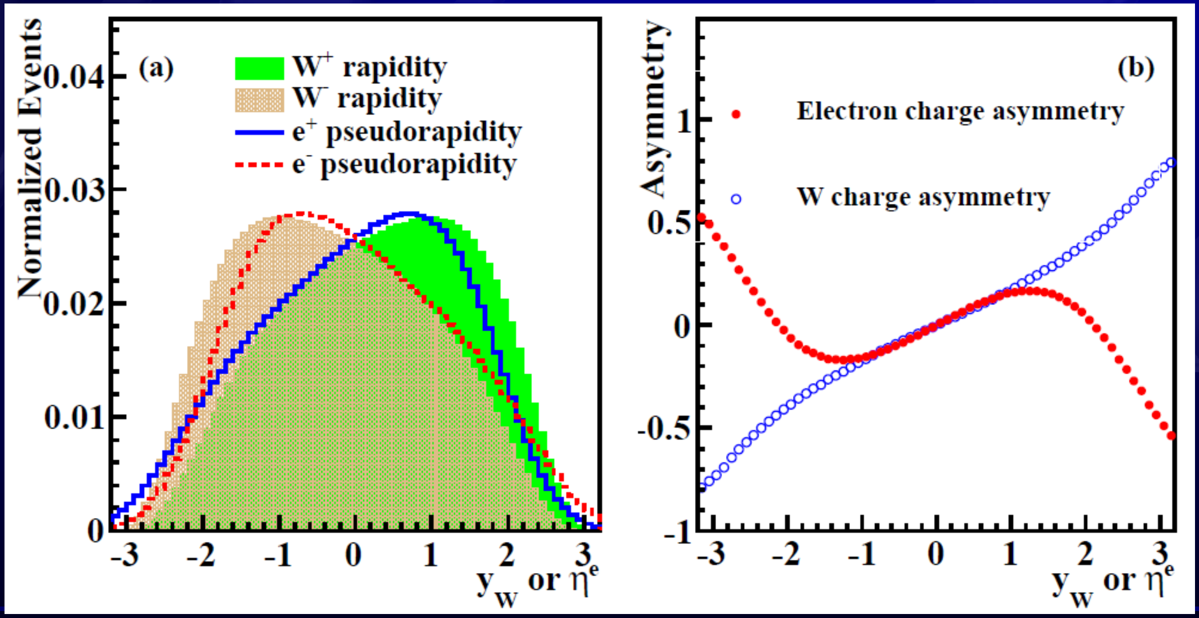

A: Strategy

- Select $W \rightarrow e\nu$ candidates from data
- Subtract backgrounds: Multijet, $Z \rightarrow ee, W \rightarrow \tau\nu, Z \rightarrow \tau\tau$
- Unfold to remove detector effects
- Use neutrino-weighting method to obtain W rapidity distributions
- Compare corrected asymmetries with theoretical predictions using different PDF sets
- Analysis performed in 5 kinematic bins:
  - Symmetric: $E_T^e > 25\ GeV$, $\cancel{E}_T > 25\ GeV$ | $35\ GeV > E_T^e > 25\ GeV$, $35\ GeV > \cancel{E}_T > 25\ GeV$ | $E_T^e > 35\ GeV$, $\cancel{E}_T > 35\ GeV$
  - Asymmetric: $35\ GeV > E_T^e > 25\ GeV$, $\cancel{E}_T > 25\ GeV$ | $E_T^e > 35\ GeV$, $\cancel{E}_T > 25\ GeV$

A: e Charge Asymmetry Results

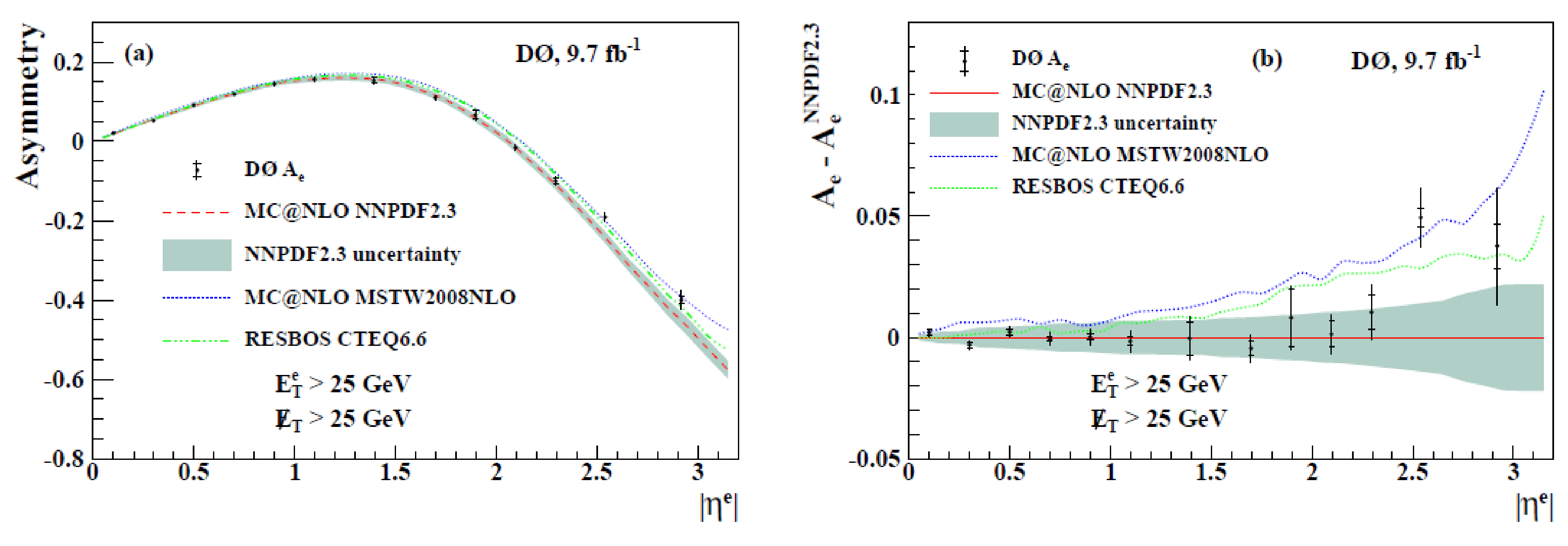

- **These results supersede previous D0 0.7 fb^{-1} measurement**
  - Old result lacked improved calibrations, e^+/e^- efficiency correction, and additional systematic uncertainties included in the current analysis

A: e Charge Asymmetry Results

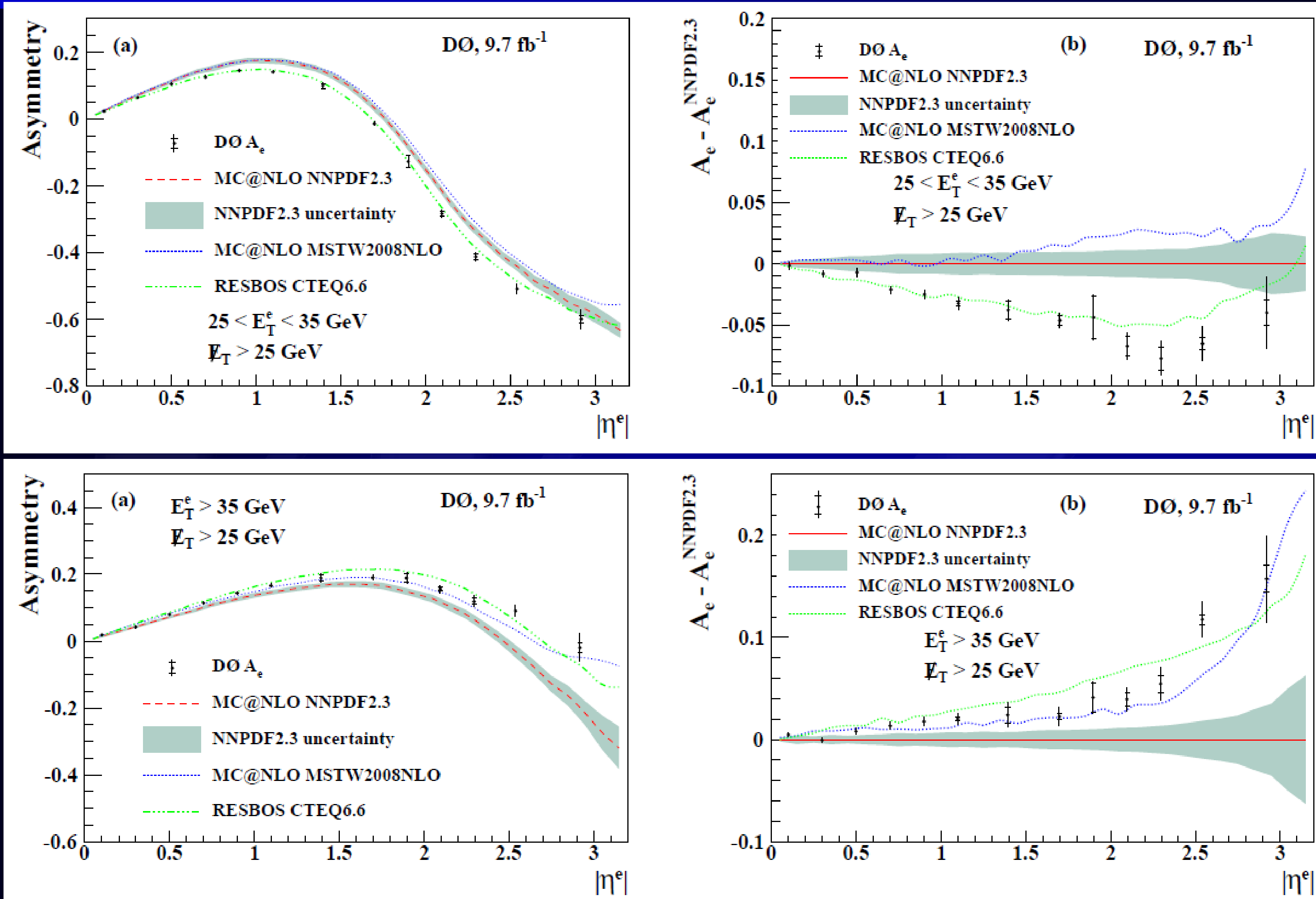

A: e Charge Asymmetry Results

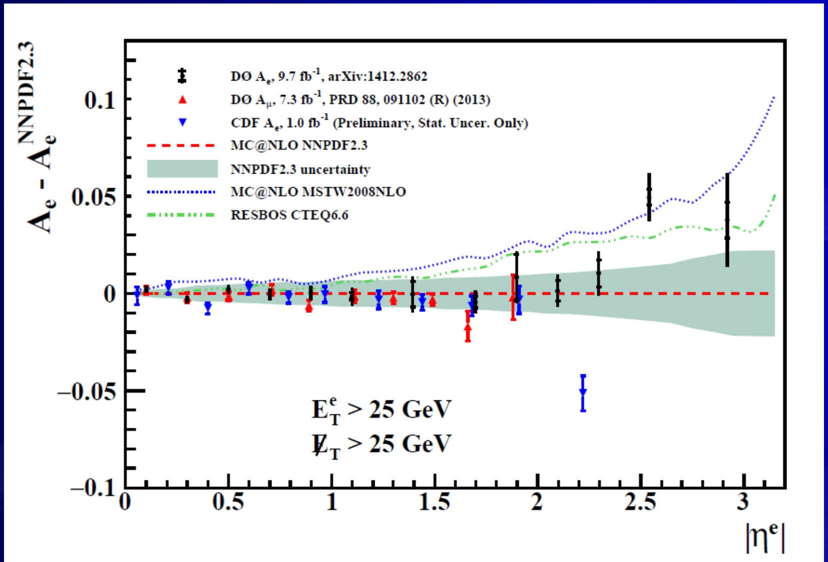

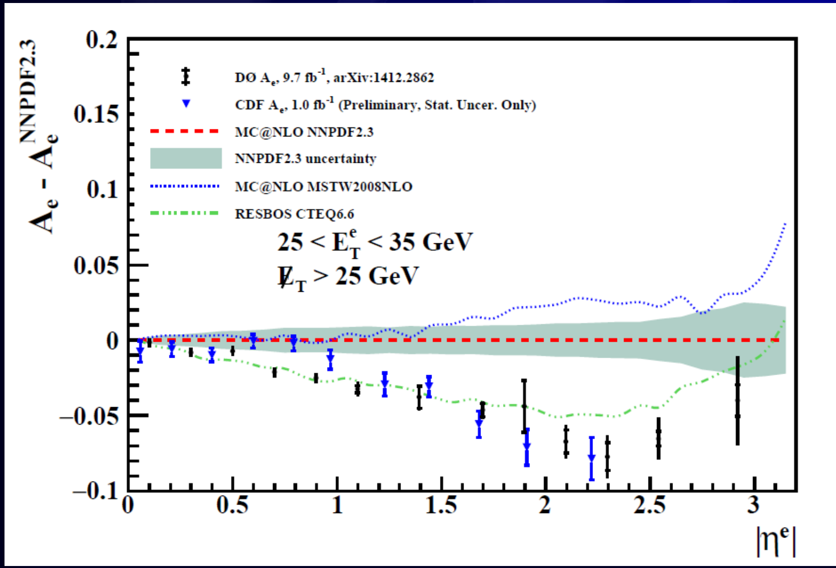

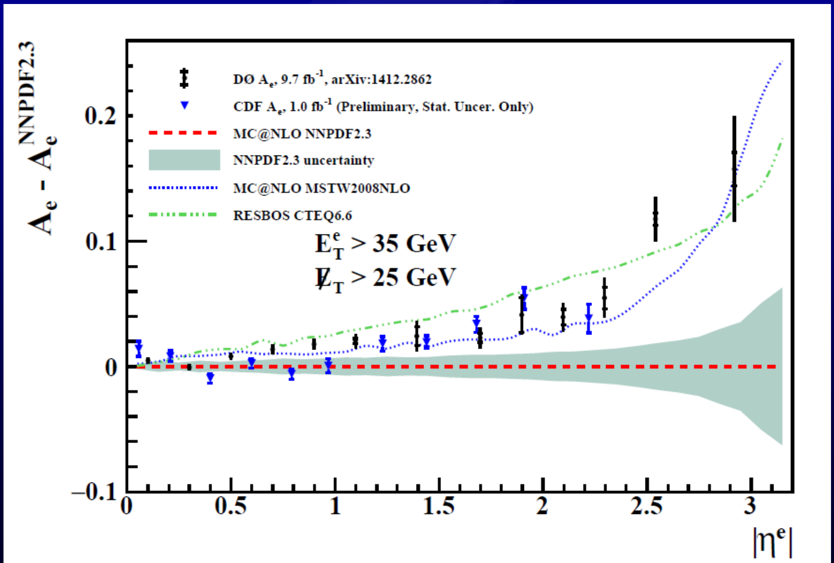

A: Summary

- **Measurement of W and electron charge asymmetry in electron channel with DØ RunII full data-set and extended η coverage to 3.2**
  - Most precise measurement of lepton charge asymmetry to date
  - Most precise direct measurement of W boson production asymmetry, and first from DØ (see backup slides)
- **Of benefit to all hadronic physics analyses**
  - Improvement of PDF models in the $x - Q^2$ region of interest for W production at the Tevatron is estimated to reduce the PDF uncertainty in the DØ M_W measurement by approximately 30% (2-3 MeV)

θ_W

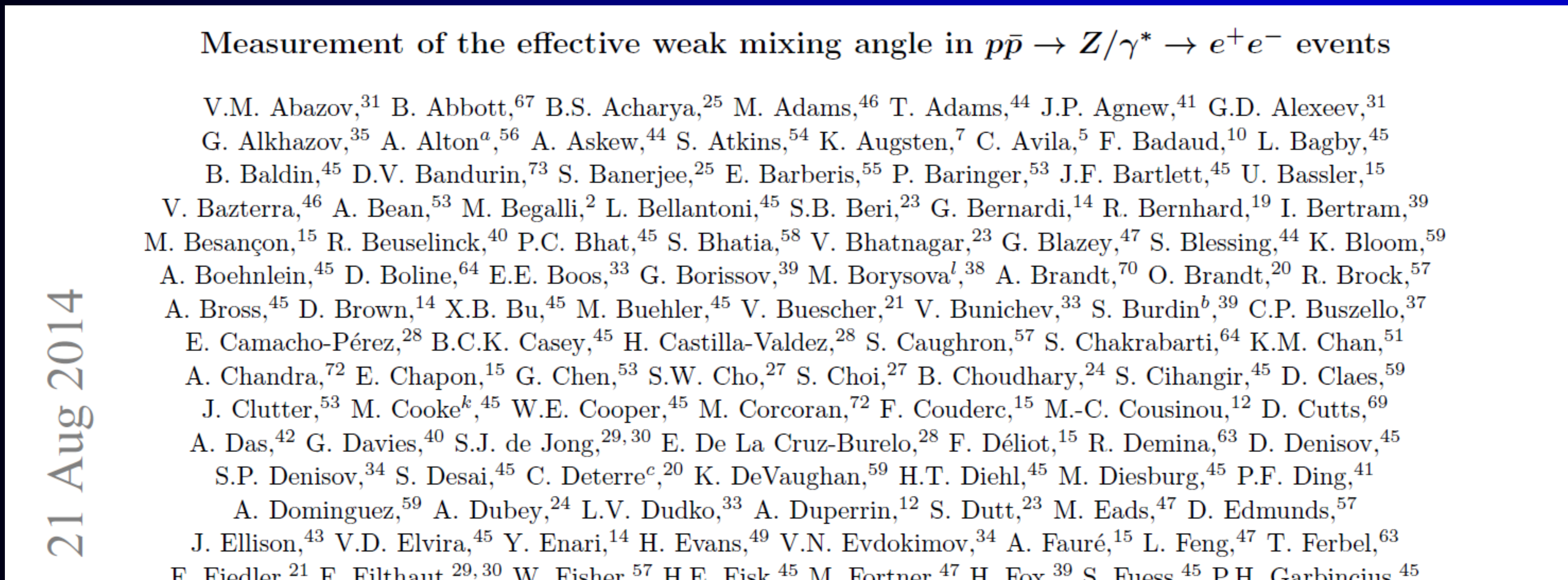

21 Aug 2014

Measurement of the effective weak mixing angle in $p\bar{p} \to Z/\gamma^* \to e^+e^-$ events

V.M. Abazov,[31] B. Abbott,[67] B.S. Acharya,[25] M. Adams,[46] T. Adams,[44] J.P. Agnew,[41] G.D. Alexeev,[31] G. Alkhazov,[35] A. Alton[a],[56] A. Askew,[44] S. Atkins,[54] K. Augsten,[7] C. Avila,[5] F. Badaud,[10] L. Bagby,[45] B. Baldin,[45] D.V. Bandurin,[73] S. Banerjee,[25] E. Barberis,[55] P. Baringer,[53] J.F. Bartlett,[45] U. Bassler,[15] V. Bazterra,[46] A. Bean,[53] M. Begalli,[2] L. Bellantoni,[45] S.B. Beri,[23] G. Bernardi,[14] R. Bernhard,[19] I. Bertram,[39] M. Besançon,[15] R. Beuselinck,[40] P.C. Bhat,[45] S. Bhatia,[58] V. Bhatnagar,[23] G. Blazey,[47] S. Blessing,[44] K. Bloom,[59] A. Boehnlein,[45] D. Boline,[64] E.E. Boos,[33] G. Borissov,[39] M. Borysova[l],[38] A. Brandt,[70] O. Brandt,[20] R. Brock,[57] A. Bross,[45] D. Brown,[14] X.B. Bu,[45] M. Buehler,[45] V. Buescher,[21] V. Bunichev,[33] S. Burdin[b],[39] C.P. Buszello,[37] E. Camacho-Pérez,[28] B.C.K. Casey,[45] H. Castilla-Valdez,[28] S. Caughron,[57] S. Chakrabarti,[64] K.M. Chan,[51] A. Chandra,[72] E. Chapon,[15] G. Chen,[53] S.W. Cho,[27] S. Choi,[27] B. Choudhary,[24] S. Cihangir,[45] D. Claes,[59] J. Clutter,[53] M. Cooke[k],[45] W.E. Cooper,[45] M. Corcoran,[72] F. Couderc,[15] M.-C. Cousinou,[12] D. Cutts,[69] A. Das,[42] G. Davies,[40] S.J. de Jong,[29,30] E. De La Cruz-Burelo,[28] F. Déliot,[15] R. Demina,[63] D. Denisov,[45] S.P. Denisov,[34] S. Desai,[45] C. Deterre[c],[20] K. DeVaughan,[59] H.T. Diehl,[45] M. Diesburg,[45] P.F. Ding,[41] A. Dominguez,[59] A. Dubey,[24] L.V. Dudko,[33] A. Duperrin,[12] S. Dutt,[23] M. Eads,[47] D. Edmunds,[57] J. Ellison,[43] V.D. Elvira,[45] Y. Enari,[14] H. Evans,[49] V.N. Evdokimov,[34] A. Fauré,[15] L. Feng,[47] T. Ferbel,[63] F. Fiedler,[21] F. Filthaut,[29,30] W. Fisher,[57] H.E. Fisk,[45] M. Fortner,[47] H. Fox,[39] S. Fuess,[45] P.H. Garbincus,[45]

Submitted to Phys. Rev. Lett. arXiv:1408.5016

08/22/14

θ_W: Theory

- **Drell-Yan lepton pairs are produced at the Tevatron through**

$$p\bar{p} \rightarrow Z/\gamma^* \rightarrow l^+l^-$$

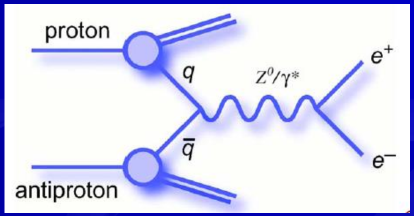

- **The weak mixing angle can be measured from the forward-backward asymmetry of the polar angle distribution of these Drell-Yan pairs**

$$\frac{q\bar{q} \rightarrow \gamma^* \rightarrow l^+l^-}{\begin{gathered} g_V^f = Q_f \\ g_A^f = 0 \end{gathered}}$$

Born level couplings

$$\langle \bar{f} | (g_V + g_A\gamma^5)\gamma^\mu | f \rangle$$

$$\frac{q\bar{q} \rightarrow Z \rightarrow l^+l^-}{\begin{gathered} g_V^f = I_3 - 2Q_f sin^2\theta_W \\ g_A^f = I_3 \end{gathered}}$$

- **I_3, $sin^2\theta_W$ couplings altered by weak radiative corrections**
  - Multiplicative factor of a few %
  - Gives effective $sin^2\theta_W$ coupling $\rightarrow$ $sin^2\theta_{eff}^l$

θ_W: Theory

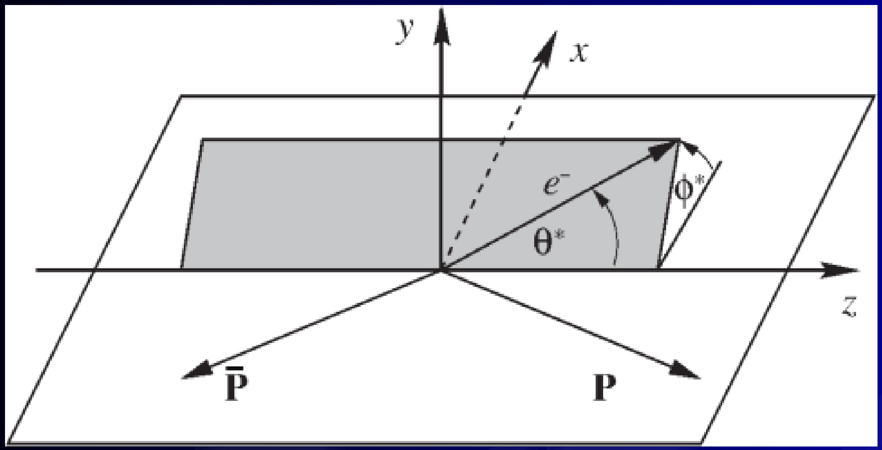

- **Measure $l^- l^+$ angular distribution in the Collins-Soper rest frame of the boson. Polar angle, θ^*, of the l^- is defined relative to the direction of the incoming quark**
  - Forward: $cos\theta^* > 0$, Backward: $cos\theta^* < 0$

$$A_{FB} = \frac{\sigma^+ - \sigma^-}{\sigma^+ + \sigma^-}$$

- Sensitive to $sin^2\theta_W$ through the interference of vector and axial vector couplings of the Z boson

θ_W: Strategy

- Measure A_{FB} in bins of lepton pair invariant mass
- Produce Monte Carlo $A_{FB}(M, sin^2\theta_W)$ templates
- Perform full corrections to data and simulation
- Extract $sin^2\theta_W$ by a χ^2 comparison between data and MC generated at different values of $sin^2\theta_W$

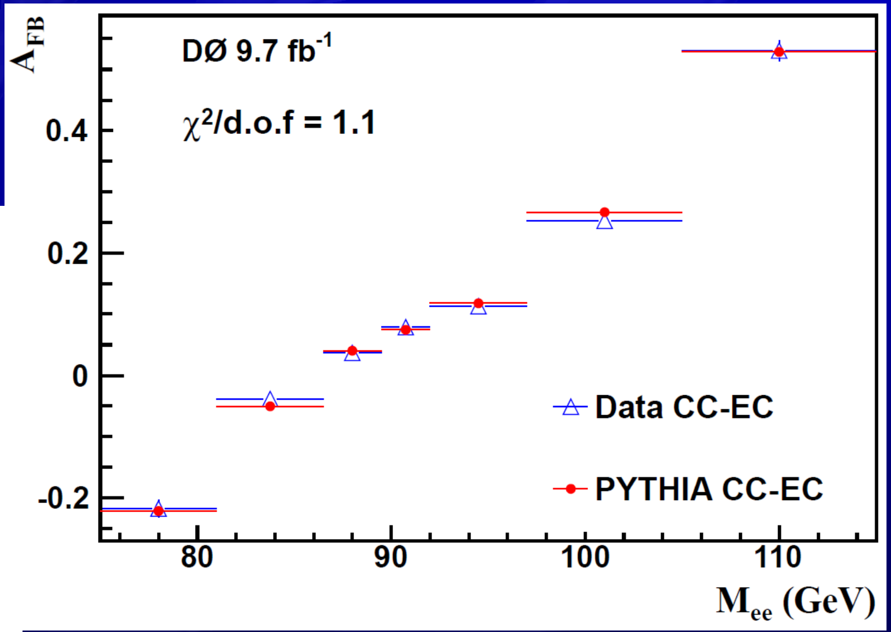

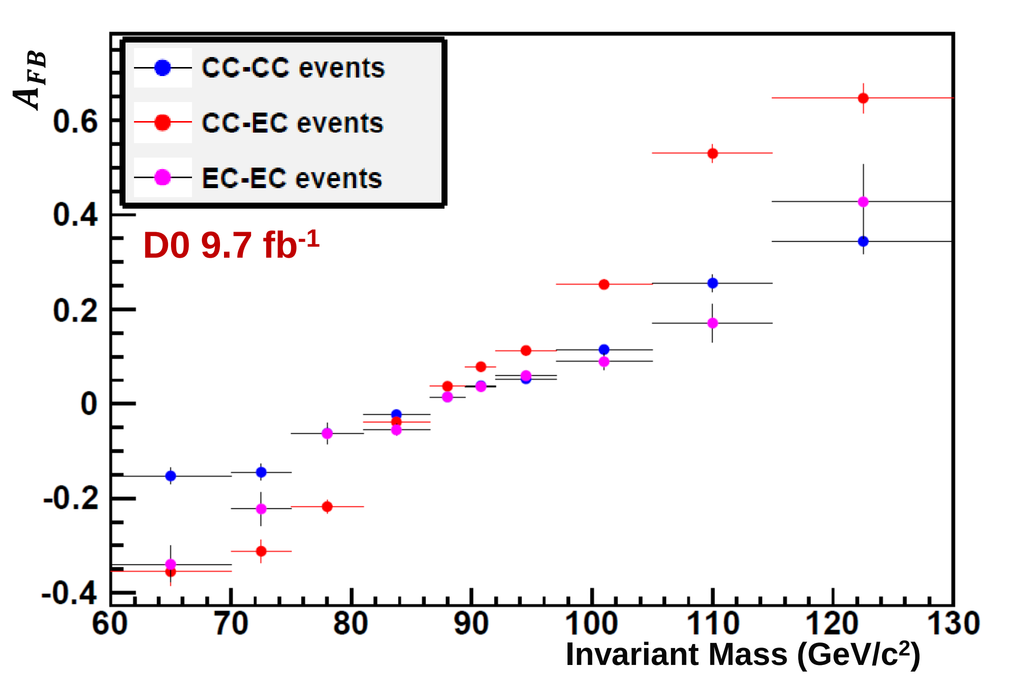

Done separately for events with both electrons in the central calorimeter (CC-CC), both in the endcaps (EC-EC), one in each (CC-EC) , and for RunIIa (1.1 fb^{-1} low L_{inst}) and RunIIb (8.6 fb^{-1} high L_{inst}) running periods

θ_W: Results

	CC-CC	CC-EC	EC-EC	Combined
$\sin^2\theta_W$	0.23142	0.23143	0.22977	0.23139
Statistical	0.00116	0.00047	0.00276	0.00043
Systematic	0.00009	0.00009	0.00019	0.00008
Energy Calibration	0.00003	0.00001	0.00004	0.00001
Energy Smearing	0.00001	0.00002	0.00013	0.00002
Background	0.00002	0.00001	0.00002	0.00001
Charge Misidentification	0.00002	0.00004	0.00012	0.00003
Electron Identification	0.00008	0.00008	0.00005	0.00007
Fiducial Asymmetry	0.00002	0.00001	0.00001	0.00001
Total	0.00116	0.00048	0.00277	0.00044

$$sin^2\theta_W = 0.23139 \underbrace{\pm 0.00043}_{\text{(stat)}} \underbrace{\pm 0.00008}_{\text{(syst)}} \underbrace{\pm 0.00017}_{\text{(PDF)}}$$

In SM context, with on-shell renormalization scheme, modified ResBos NLO correction

$$\boxed{sin^2\theta^l_{eff} = 0.23147 \pm 0.00047}$$

(thanks to Willis Sakumoto for help)

World's Best From Hadron Collider & from Light Quark Interactions

θ_W: Summary

- D0 9.7 fb^{-1} : $sin^2\theta^l_{eff} = 0.23147 \pm 0.00047$
- World's best from hadron collider
- PRD with full A_{FB} and coupling details in preparation
  - Including indirect M_W determination

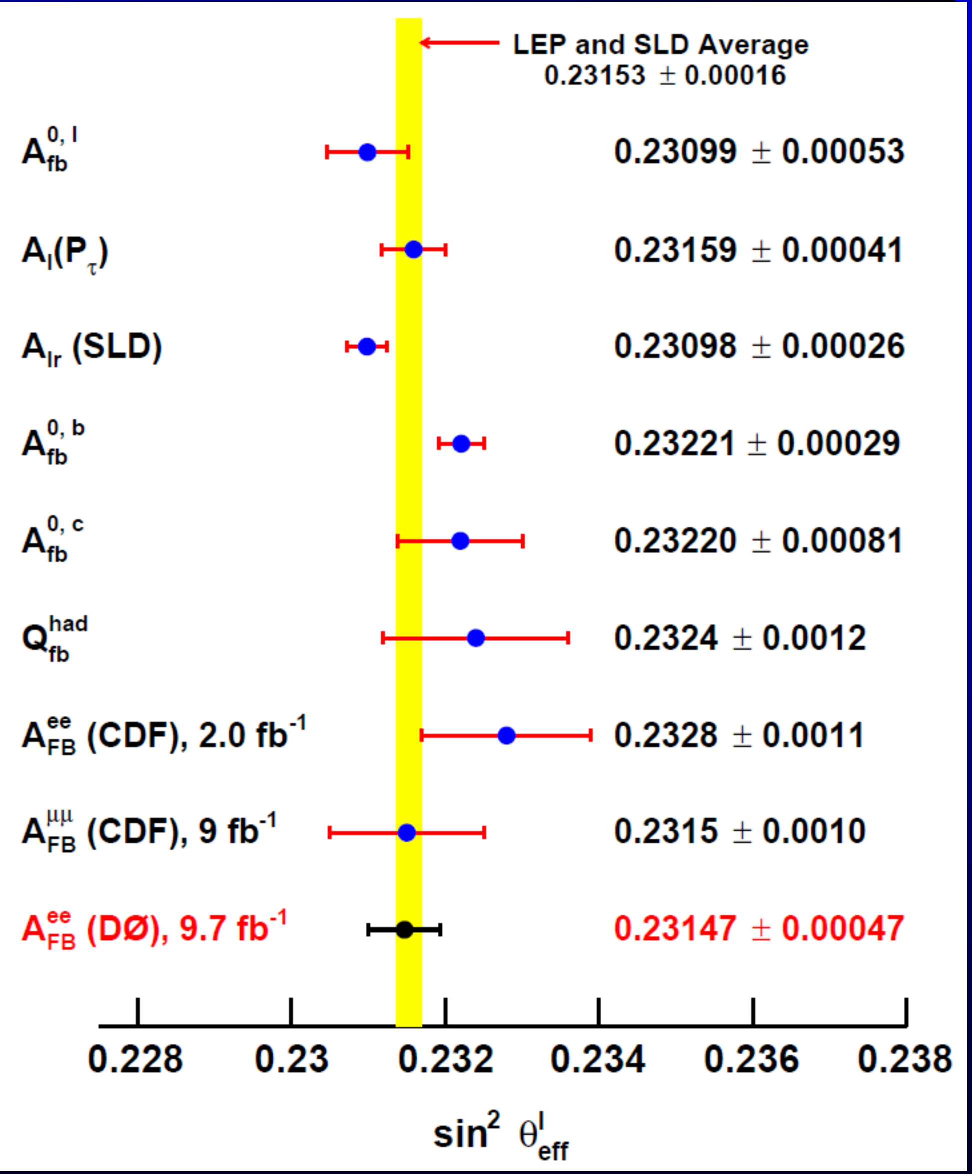

Conclusions

- WW+jets : **First differential cross section for massive dibosons**
- ϕ^*: **New high-precision observable, first ever transverse momentum results in off-peak regions**
- A: **Highest precision *W* and *e* charge asymmetry results extended to higher η, Tevatron data consistent and discrepant from many models+PDFs**
- θ_W: **World's best result from hadron collider and light quark interactions**

For more analysis detail see backup slides and
11/11/14 Fermilab Wine & Cheese

- ***More to come***!
  - e.g. Tevatron combination of full data $sin^2\theta_W$ in electron and muon channels

Backup Slides

The Tevatron

- **Great thanks to Accelerator Division for all the luminosity!!**

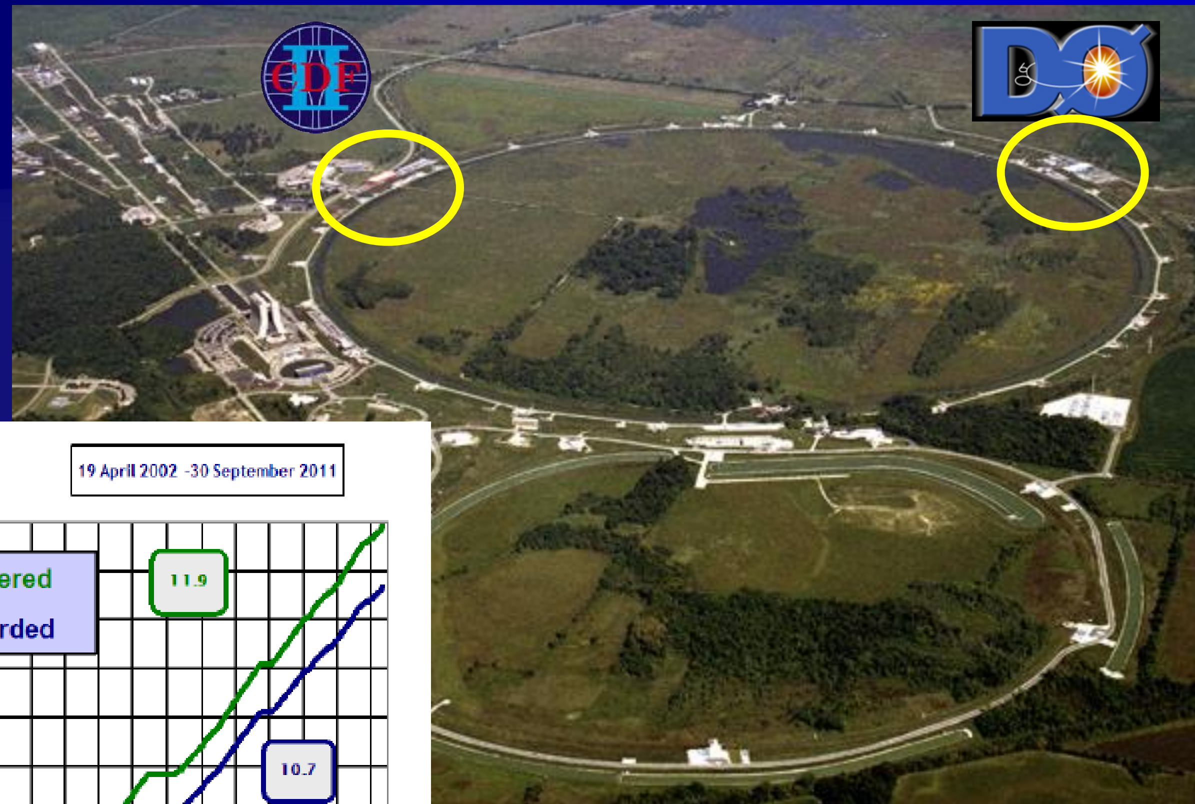

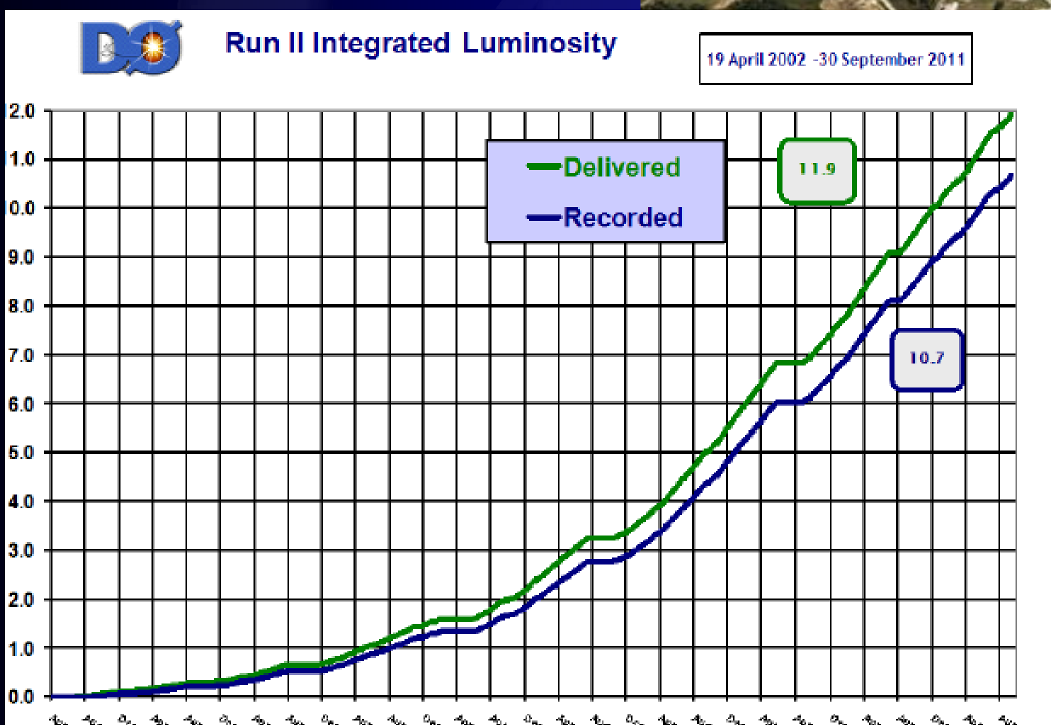

W^+W^- Data, MC

Signal regions

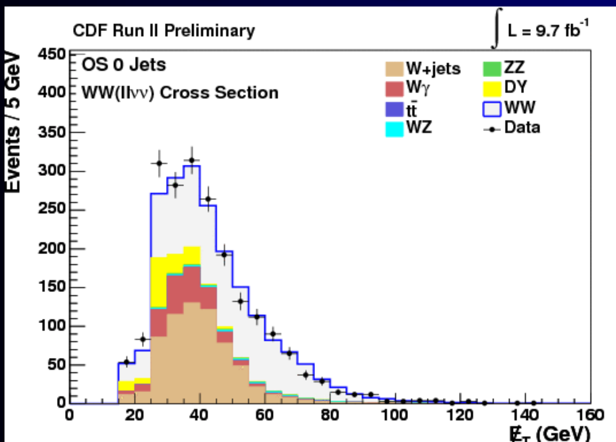

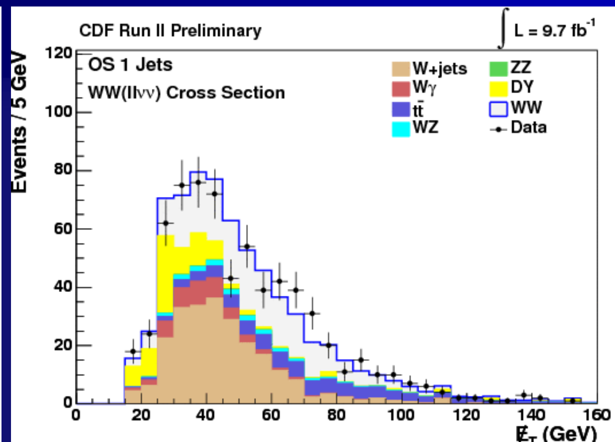

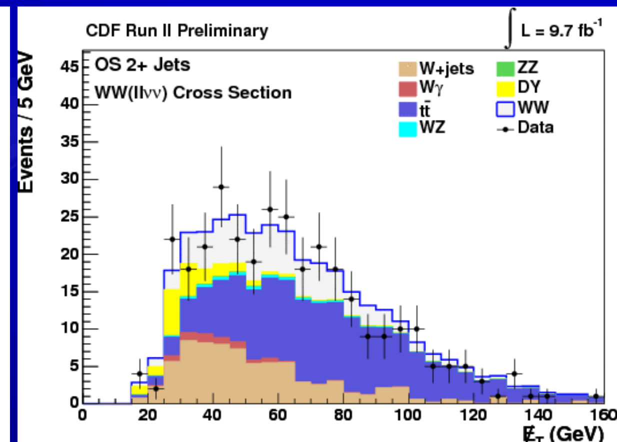

Control regions

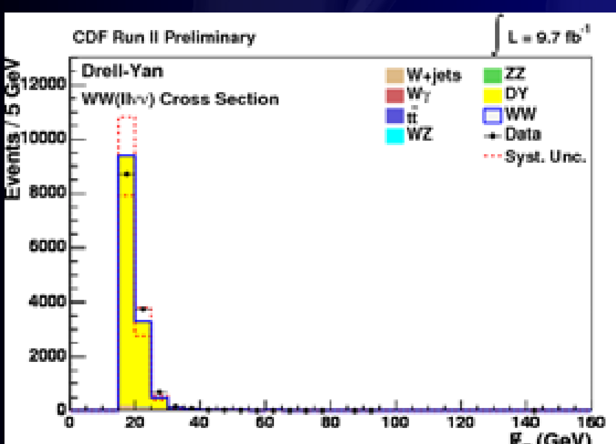

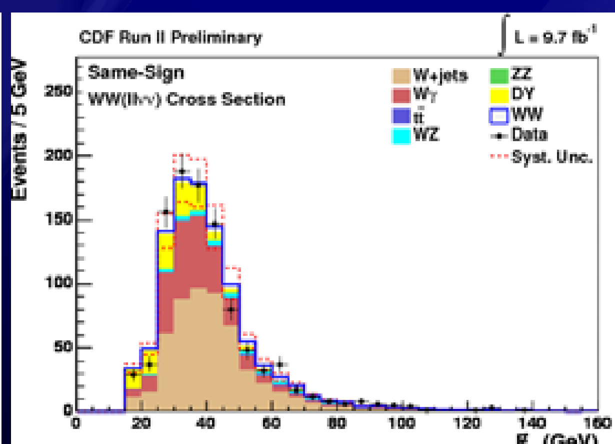

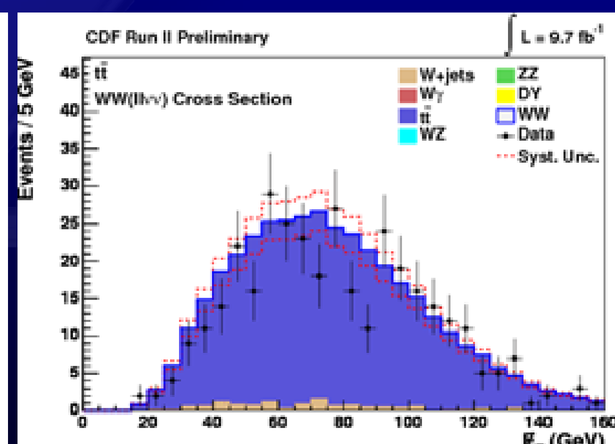

W^+W^- Template fits

- Neural net output distribution fits for each bin

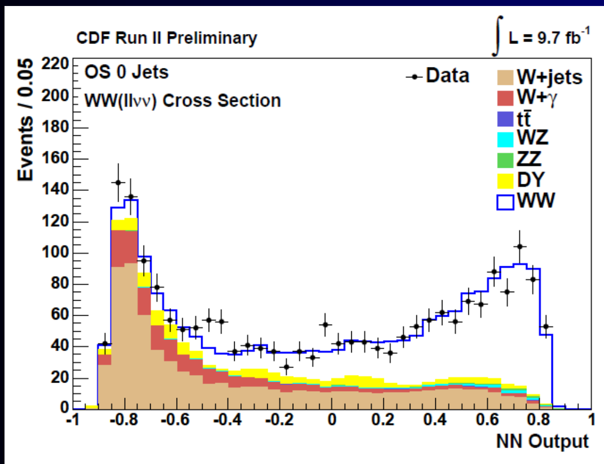

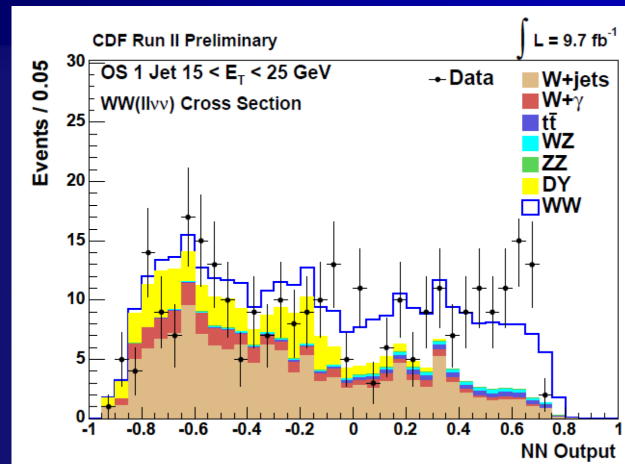

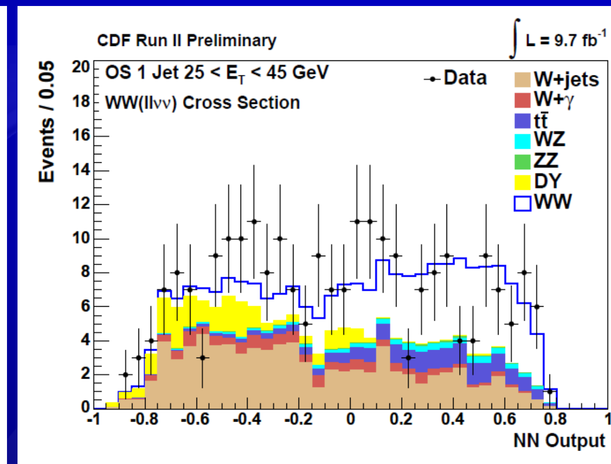

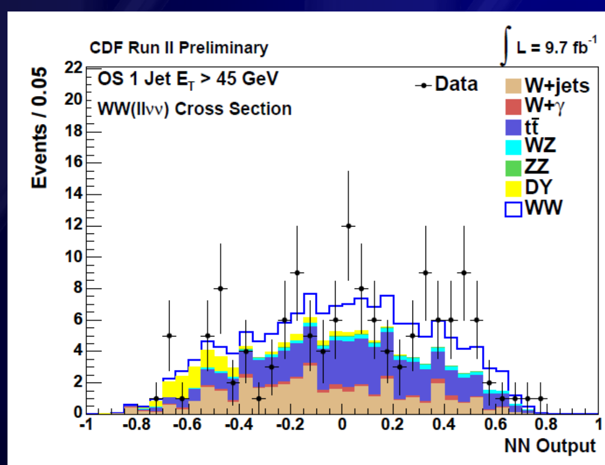

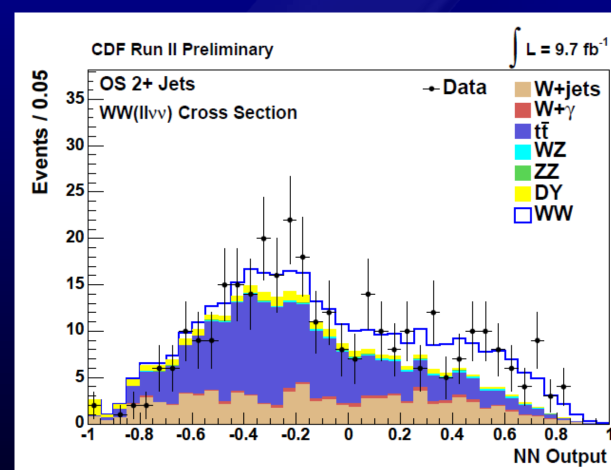

W^+W^- Systematic Uncertainties

- Systematic uncertainties for the 0 jet analysis bin

WW(ll$\nu\nu$) Cross Section	0 Jets			CDF Run II Preliminary		$\int \mathcal{L} = 9.7$ fb^{-1}	
Uncertainty Source	WW	WZ	ZZ	$t\bar{t}$	DY	$W\gamma$	W+jet
Cross Section	6.0%	6.0%	6.0%	4.3%*			
Acceptance							
$\not\!\!E_T$ Modeling					19.0%*		
Higher-order Diagrams		10.0%	10.0%			10.0%*	
$t\bar{t}$ QCD				2.7%			
Conversion Modeling						6.8%	
Scale	3.8%						
PDF Modeling	0.8%						
Jet Energy Scale	4.7%	6.4%	3.5%	26.8%	10.2%	3.5%	
Lepton ID Efficiencies	3.8%	3.8%	3.8%	3.8%	3.8%		
Trigger Efficiencies	2.0%	2.0%	2.0%	2.0%	2.0%		
Jet Fake Rate							17.2%
Luminosity	5.9%	5.9%	5.9%	5.9%	5.9%		

* indicates uncorrelated systematic. (−) indicates anticorrelated systematic.

Impacts of PDFs

Source	Public. 2009 (1.0 fb^{-1})	Public. 2012 (4.3 fb^{-1})	Proj. 10 fb^{-1}	Proj. 10 fb^{-1} improv.	Proj. 10 fb^{-1} improv. + EC
Statistical	23	13	9	9	8
Experimental syst.					
Electron energy scale	34	16	11	11	10
Electron energy resolution	2	2	2	2	2
EM shower model	4	4	4	2	2
Electron energy loss	4	4	4	2	2
Hadronic recoil	6	5	3	3	2
Electron ID efficiency	5	1	1	1	1
Backgrounds	2	2	2	2	2
Subtotal experimental syst.	35	18	13	12	11
***W* production and decay model**					
PDF	9	11	11	11	5
QED	7	7	7	3	3
boson p_T	2	2	2	2	2
Subtotal W model	12	13	13	12	6
Total systematic uncert.	37	22	19	17	13
Total	**44**	**26**	**21**	**19**	**15**

combination: 23

ϕ*: Peak Region

- First measured by D0 with 7.3 fb^{-1}
  - PRL 106, 122001 (2011)

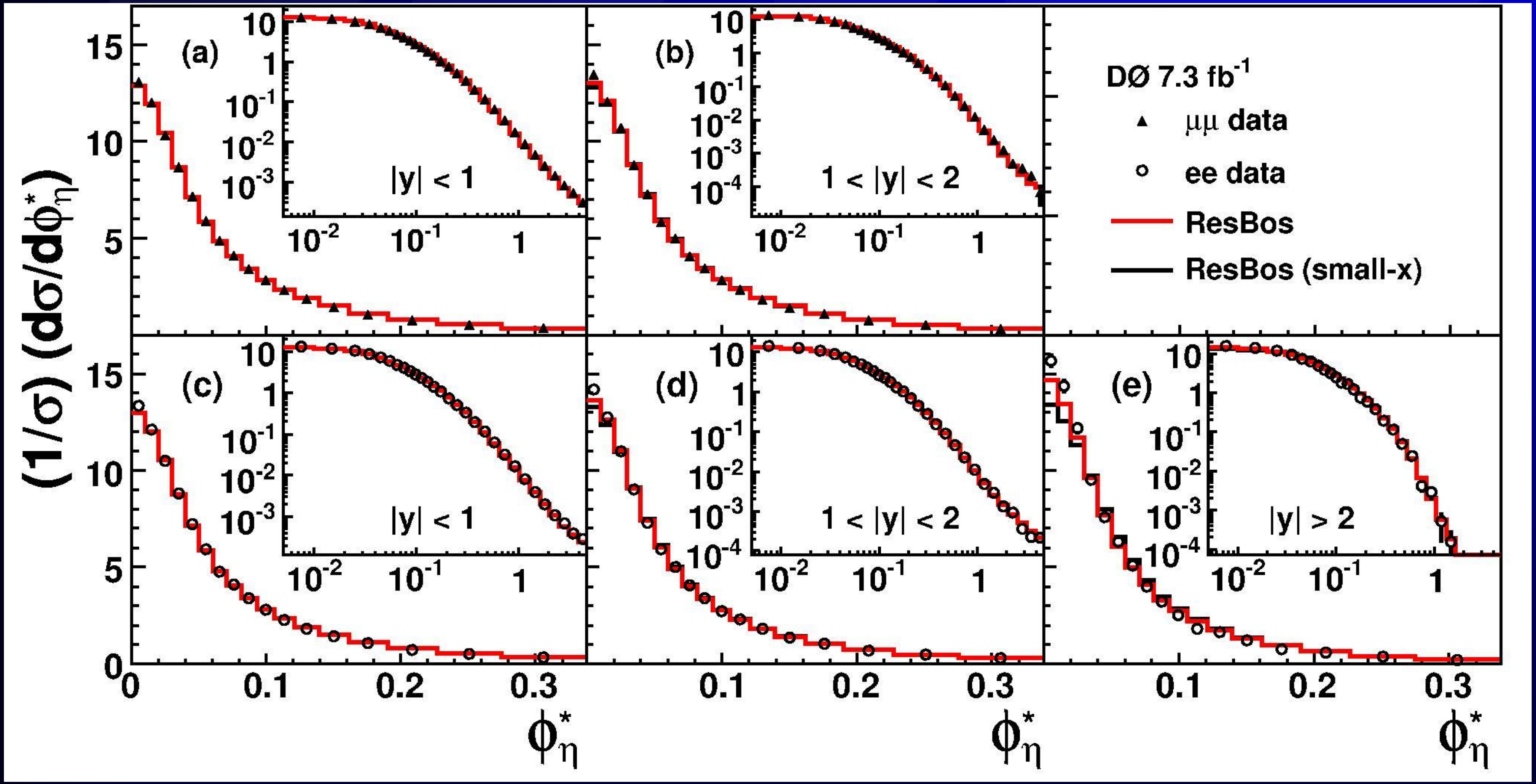

ϕ^*: Peak Region

- First measured by D0 with 7.3 fb^{-1}
  - PRL 106, 122001 (2011)

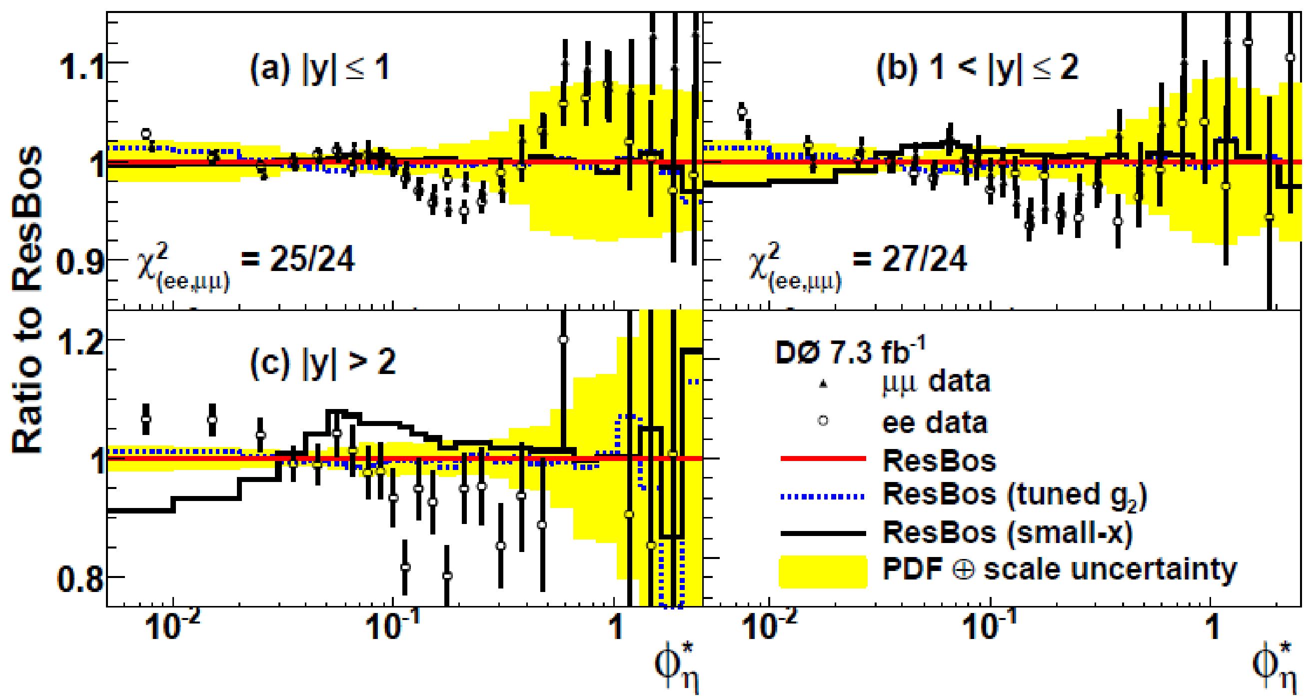

Figure: $M_{\mu\mu} \in (70, 110)$

- Data used to improve ResBos and make predictions for LHC

ϕ^*: Event Selection

- **Select events with two good quality muons (isolation, track segments, vertex)**
  - Tighter quality cuts for low mass region to control backgrounds

- **Peak region**
  - $M_{\mu\mu} \in (70,110)$ GeV:
  - 645k events with 99.84% signal

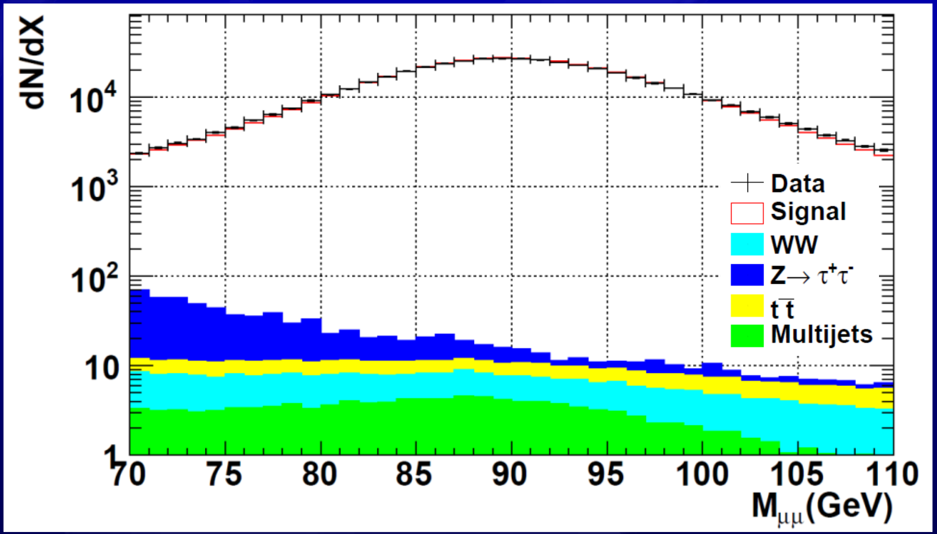

- **Low mass region**
  - $M_{\mu\mu} \in (30,60)$ GeV
  - 74k events with 89.5% signal
- **High mass region**
  - $M_{\mu\mu} \in (160,300)$ GeV: 1.7k events with 72.8% signal
  - $M_{\mu\mu} \in (300,500)$ GeV: 0.2k events with 56.6% signal

ϕ^*: High Mass Region Results

- **First ever high-mass region results (2k events)**
  - Constrain initial state QCD radiation uncertainties for high mass final states
    - e.g. top quark physics
  - No detailed comparison can be made due to limited statistics.

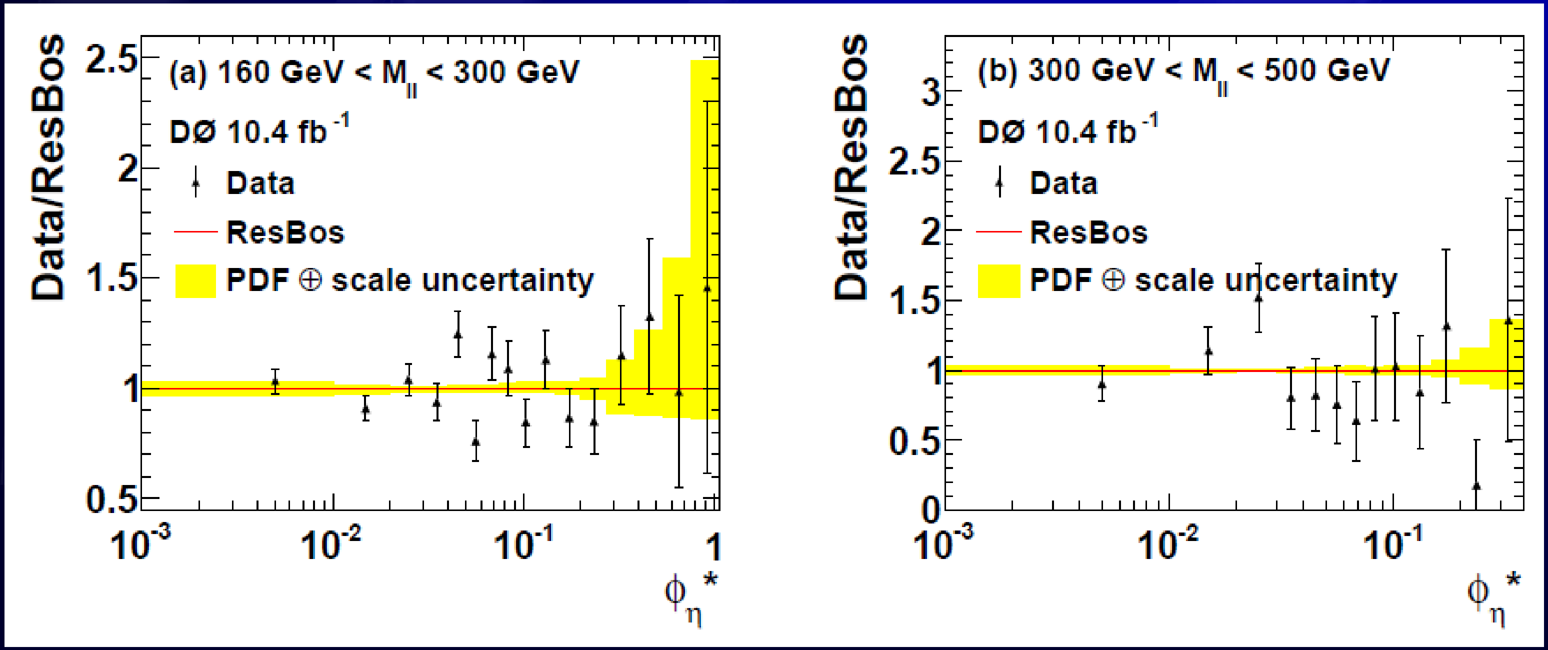

A: Introduction

- Asymmetry vs. x : the lepton asymmetry comes from a larger range of parton x values compared with the W asymmetry
- The W asymmetry is more sensitive to the u/d ratio

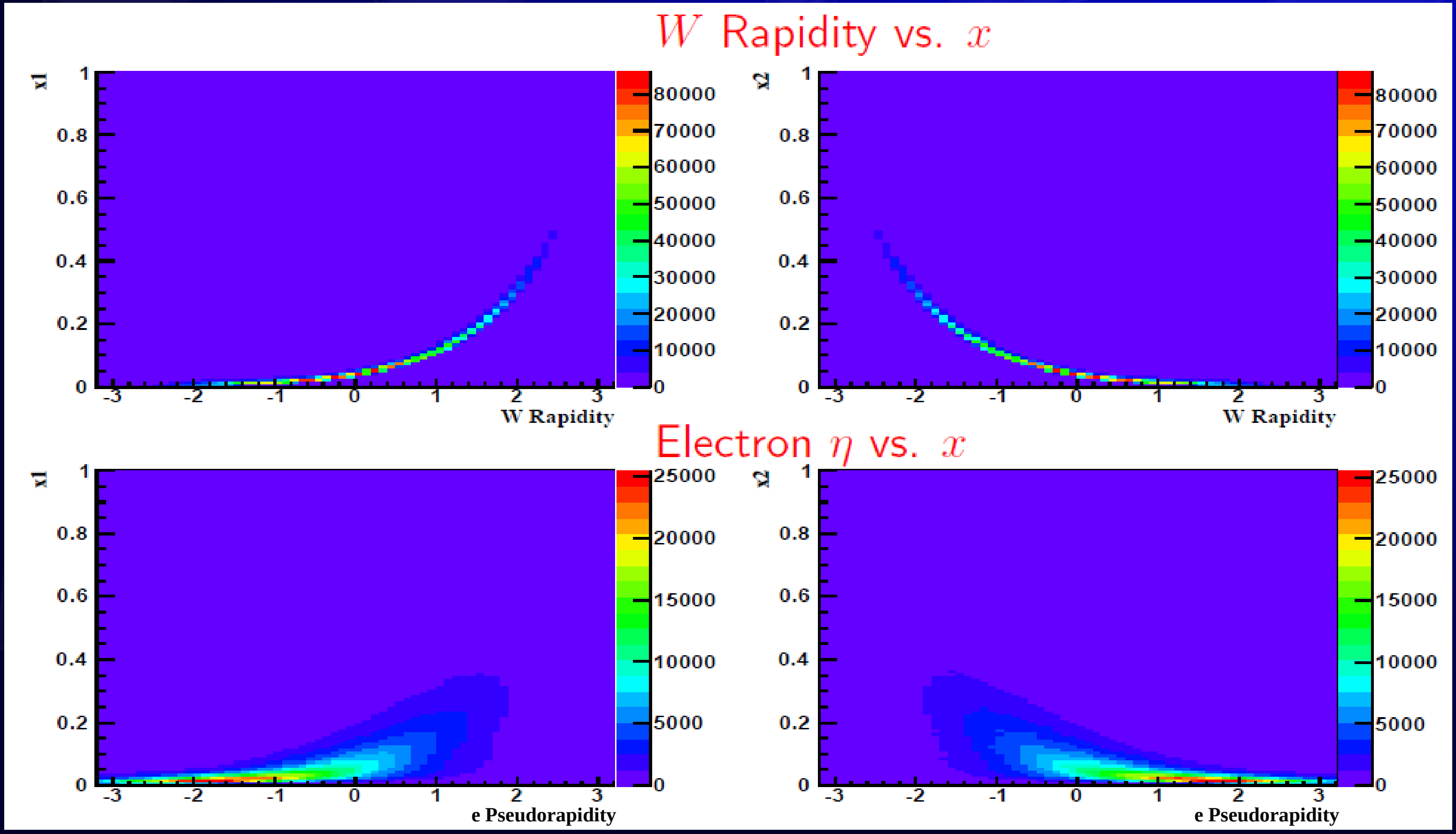

A: Selection and Backgrounds

- **Event Selection (full data, 9.7 fb^{-1})**
  - Electron: $25 < p_T < 100$ GeV
  - Missing transverse energy > 25 GeV
  - W: $50 < M_T < 130$ GeV
  - Track matching
- **Backgrounds**
  - QCD: 4.0%
  - $Z \to ee$: 2.6%
  - $W \to \tau\nu$: 2.2%
  - $Z \to \tau\tau$: 0.2%

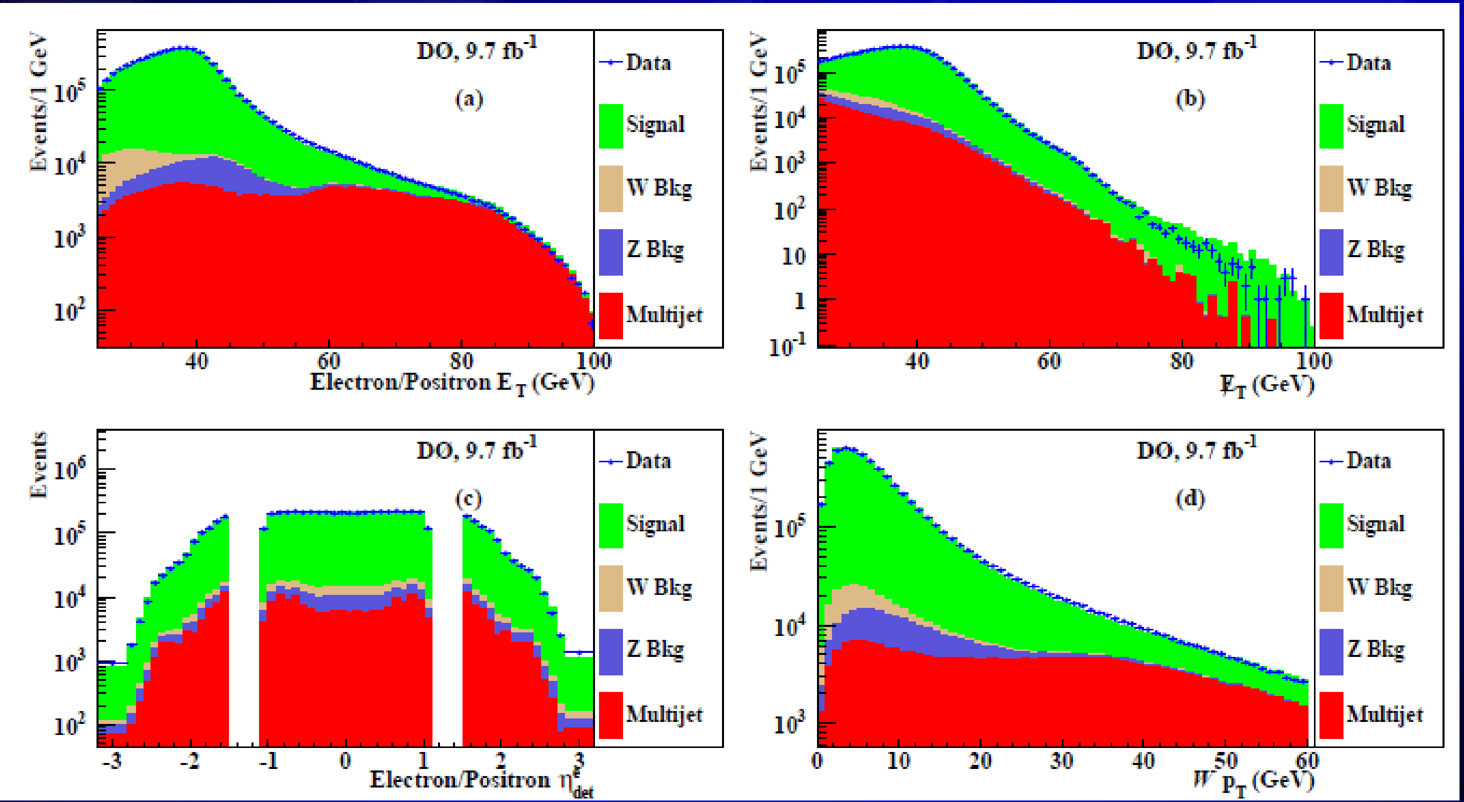

A: Unfolding

1. **Migration matrix: used to remove detector resolution effects**
   - Electron and positron are expected to have same detector response
   - Study migration matrices for all events ($e^- + e^+$): no input bias
2. **$K^{\pm}_{eff}$: relative efficiency for positrons and electrons**
   - Use $Z \rightarrow ee$ events to study $K^{\pm}_{eff}$ track bias from alignment + solenoid polarity
   - Only study $K^{\pm}_{eff}$ for track cuts, do not expect calorimetry cuts to have such effects
3. **Acc × Eff: to remove kinematic and geometric cut effects**

A: Neutrino weighting for W

A. Bodek, et. al. PRD 77, 111301(R) (2008)

- **W rapidity:**
  - Massive particle rapidity: $y = \frac{1}{2} ln \frac{E+p_Z}{E-p_Z}$
  - Fix M_W to 80.385 GeV, $M_W^2 = (E_l + E_\nu)^2 - \left(\overrightarrow{P_l} + \overrightarrow{P_\nu}\right)^2$
- **Obtain neutrino p_Z^ν solutions, with given mass of W:**
  - If there are two complex solutions, which means $\not{E}_T$ is not measured properly, we scale the $\not{E}_T$ to set the imaginary part to 0
  - If two solutions, give each solution a weight factor, according to W p_T, Collins angle, and rapidity of W boson:

$$P_\pm\left(\cos\theta^*, y_W, p_T^W\right) = \left(1 \mp \cos\theta^*\right)^2 + Q\left(y_W, p_T^W\right)\left(1 \pm \cos\theta^*\right)^2$$

$$w_{1,2}^\pm = \frac{P_\pm\left(\cos\theta_{1,2}^*, y_{1,2}, p_T^W\right) d\sigma^\pm\left(y_{1,2}\right)}{P_\pm\left(\cos\theta_1^*, y_1, p_T^W\right) d\sigma^\pm\left(y_1\right) + P_\pm\left(\cos\theta_2^*, y_2, p_T^W\right) d\sigma^\pm\left(y_2\right)}$$

A: Closure Tests

- Half of MC used for input, half for pseudo-data

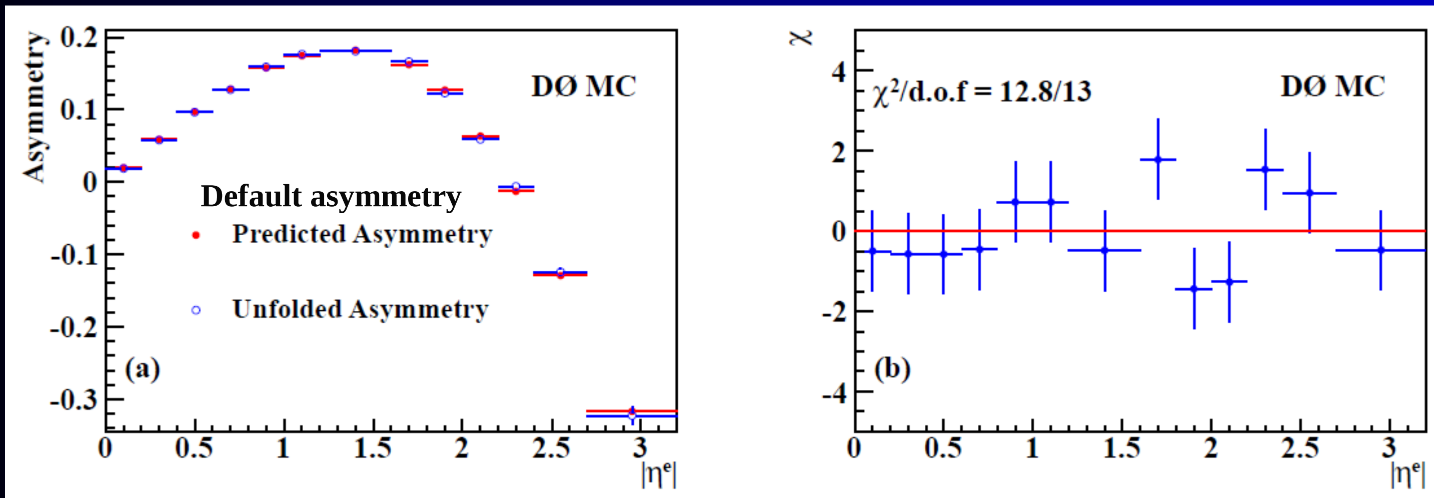

- We get out what we put in

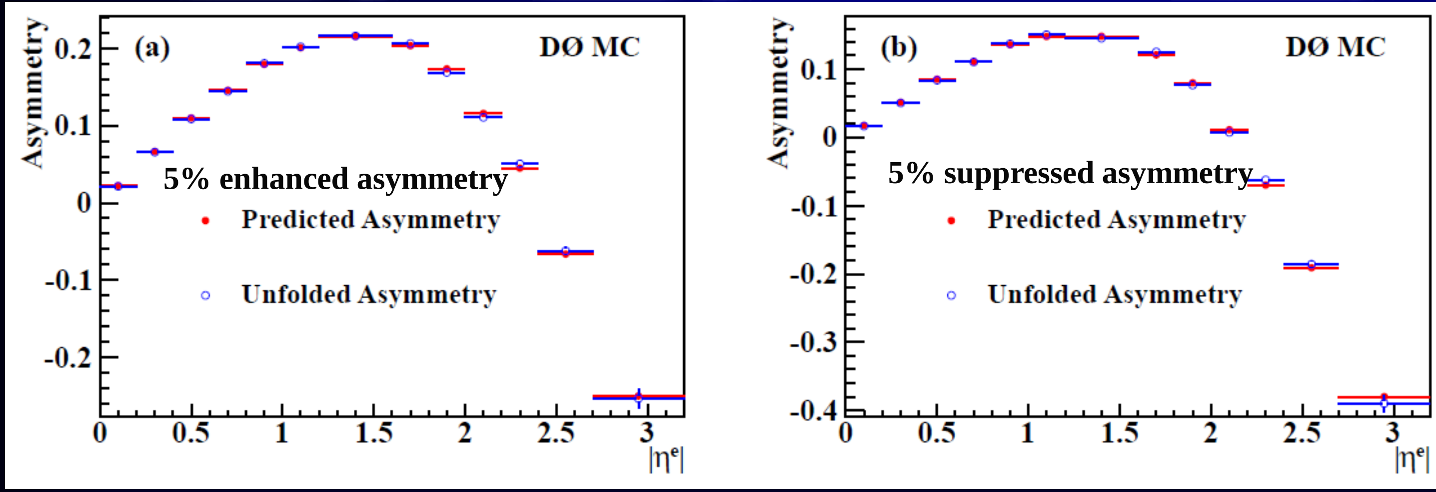

- Unfolding corrections valid for range of asymmetry

A: e Charge Asymmetry Results

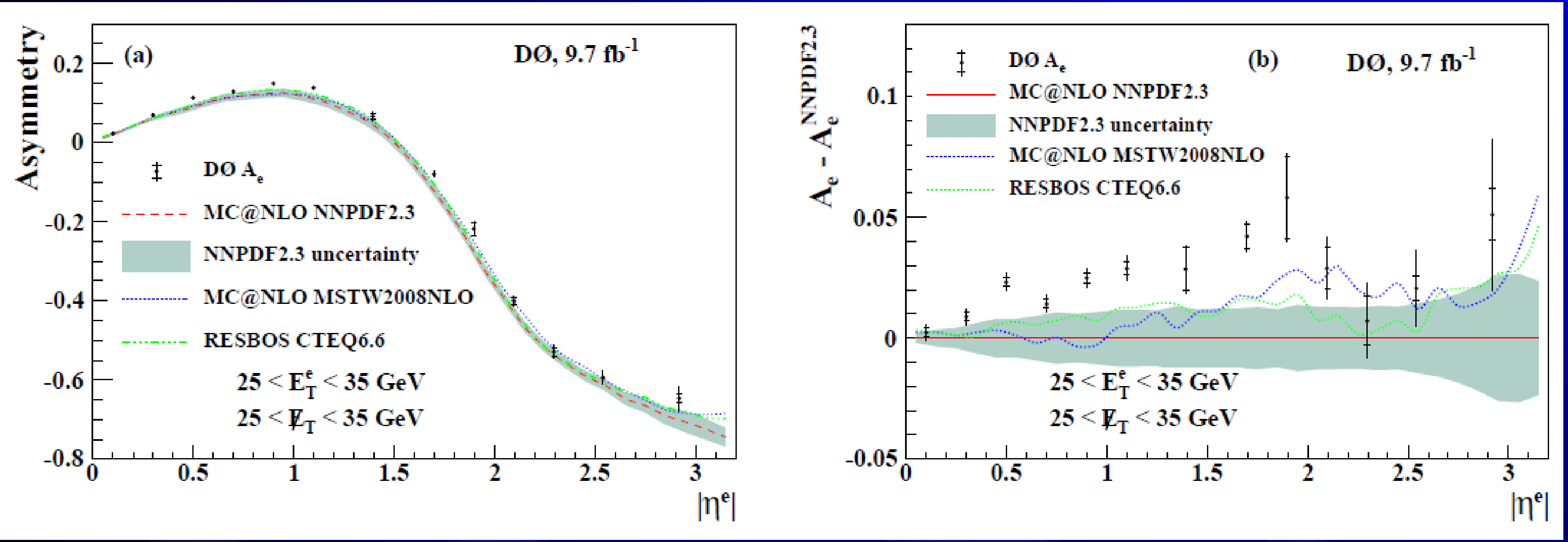

A: e Charge Asymmetry Results

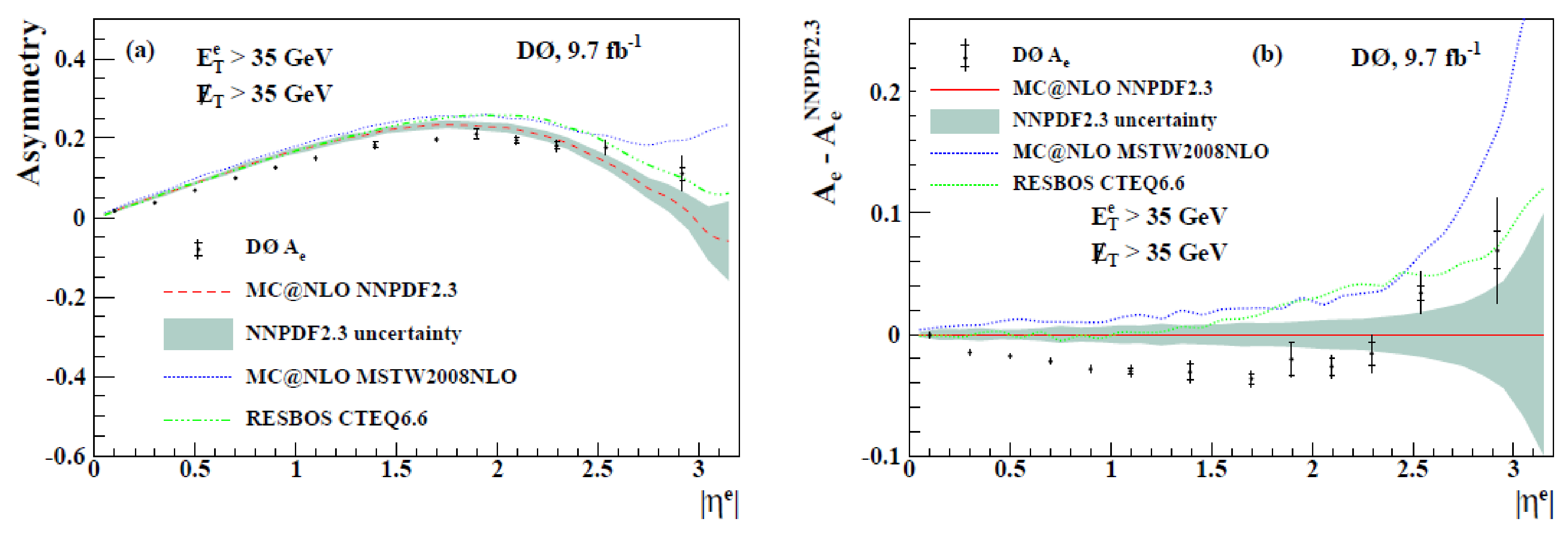

A: W Charge Asymmetry Result

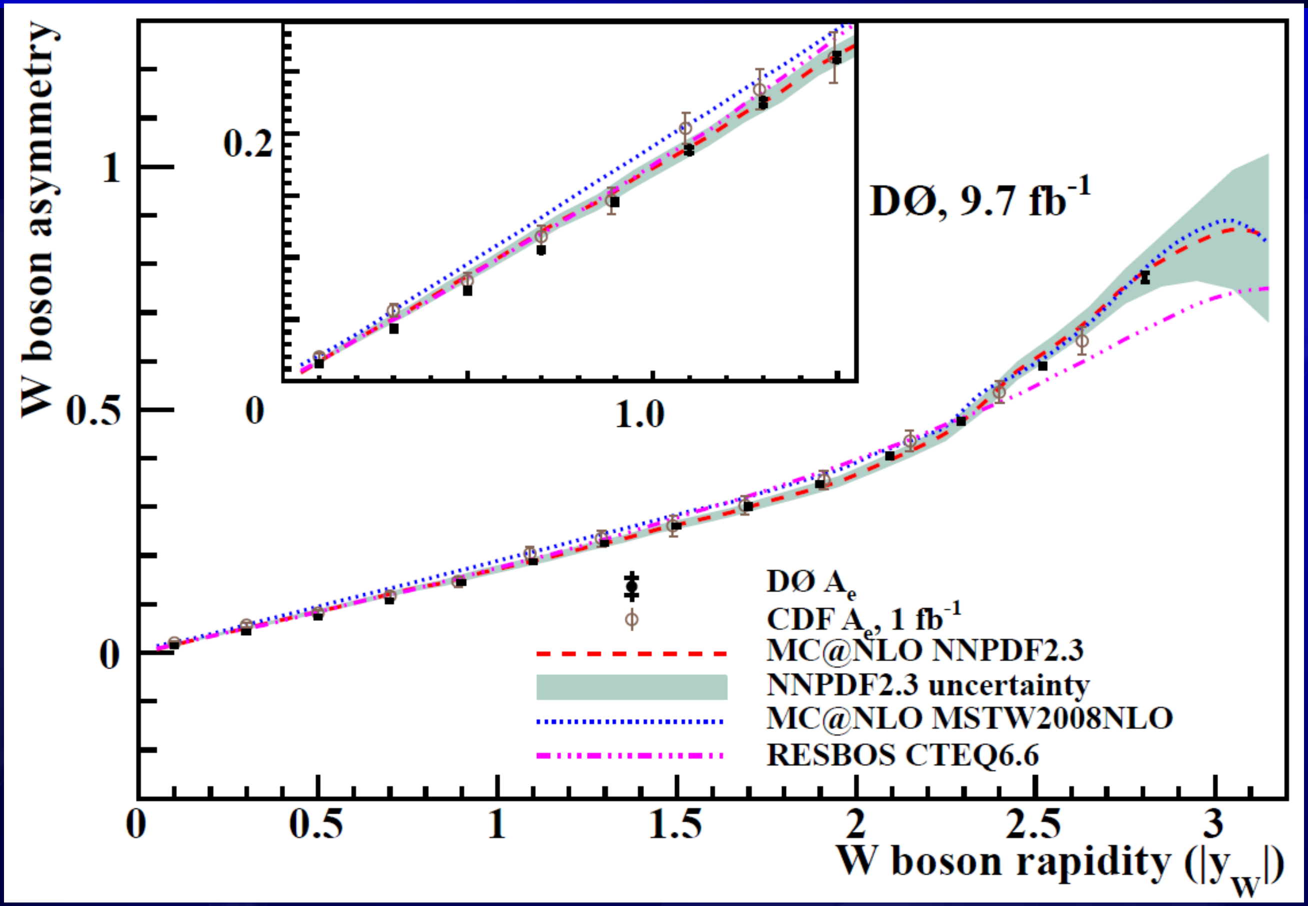

- **Erratum to PRL 112, 151803 (2014) arXiv:1312.2895**
  - Now employing corrected $K_{eff}^{\pm}$ determination from e charge asymmetry
  - < 2% difference from original publication

θ_W: Theory

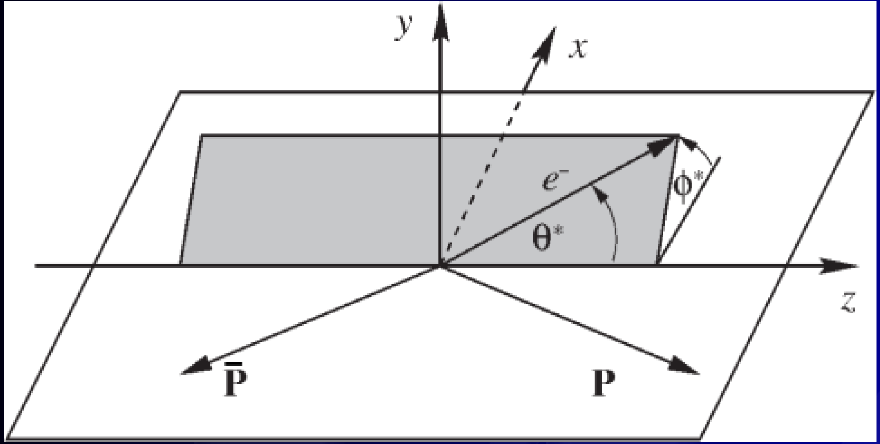

- **Measure l^-l^+ angular distribution in the Collins-Soper rest frame of the boson. Polar angle, θ^*, of the l^- is defined relative to the direction of the incoming quark**
  - Forward: $cos\theta^* > 0$, Backward: $cos\theta^* < 0$

- $dN/d\Omega \propto 1 + cos^2\theta^* + A_4 cos\theta^*$
  - All coefficients† but A_4 vanish as $P_T \rightarrow 0$

$$A_{FB} = \frac{\sigma^+ - \sigma^-}{\sigma^+ + \sigma^-} = \frac{3}{8}A_4$$

- $A_4 cos\theta^*$**: parity violating, from interference of vector and axial vector currents**
  - Sensitive to $sin^2\theta_W$ through Z self-interference: $(1 - 4|Q_l|sin^2\theta_W)(1 - 4|Q_q|sin^2\theta_W)$

†@ NLO QCD: $dN/d\Omega = 1 + cos^2\theta^* + A_0(1 - 3cos^2\theta^*)/2 + A_1 sin2\theta^* cos\phi + A_2(sin^2\theta^* cos2\phi)/2 + A_3 sin\theta^* cos\phi + A_4 cos\theta^* + A_5 sin^2\theta^* sin2\phi + A_6 sin2\theta^* sin\phi + A_7 sin\theta^* sin\phi$

θ_W: Event Selection

- **Full D0 RunII dataset: 9.7 fb^{-1}**
- **Two high-P_T electrons: $P_T > 25$ GeV**
  - Central and endcap calorimeters (CC,EC)
- **Tight track requirements**
- **Mass distribution: $M > 50$ GeV**
  - $\sin^2\theta^l_{eff}$ from $75 < M < 115$ GeV
- **85% increase in statistics**
  - Extend to $|\eta| < 1.1, 1.5 < |\eta| < 3.2$
  - Include EC-EC events
  - Include electrons near calorimeter module (phi-mod) boundaries
  - Track reconstruction improvements
- **560,267 events**
- **Low QCD backgrounds (EW negl.)**
  - CC-CC: 0.4%; CC-EC,EC-EC: < 4%
- **MC: PYTHIA, CTEQ6L1**

- CC-CC: both electrons in the central calorimeter
- CC-EC: one electron in the central calorimeter, the other in an endcap
- EC-EC: both electrons in the endcap calorimeters

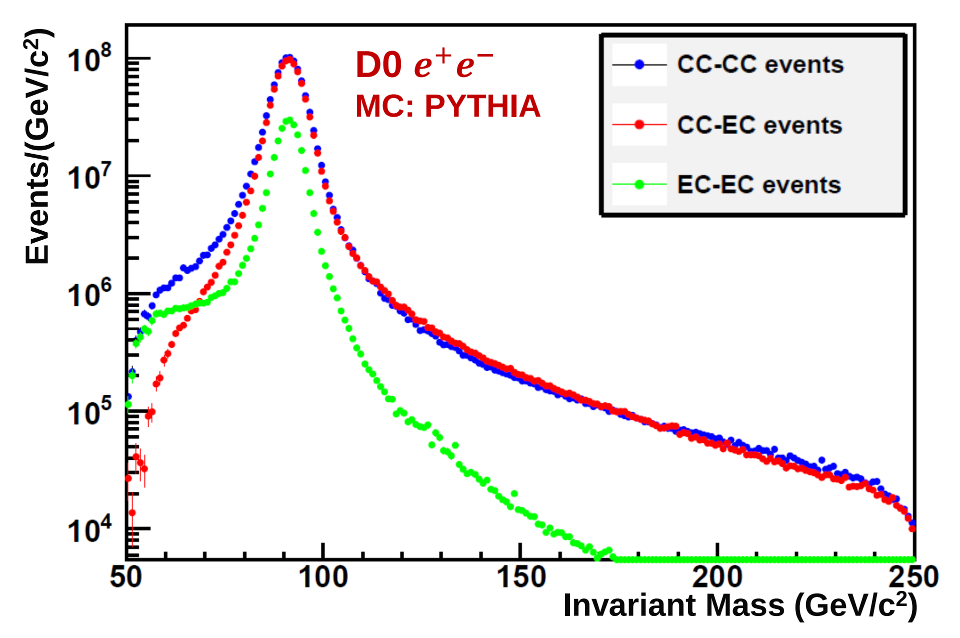

θ_W: Energy Calibration

- **Global energy scale modeling in previous analysis**
  - Shape dependence inadequate for different detector responses of extended acceptance regions
- **New method corrects energy as a function of L_{inst} first, then η_{det}**
  - Z mass peak scaled to LEP value (91.1875 GeV) in each bin
  - Separate calibrations for data and MC
- **After calibration, mass peak L_{inst} dependence negligible, η_{det} dependence reduced from 2 GeV to 100 MeV (data), 10 MeV (MC)**

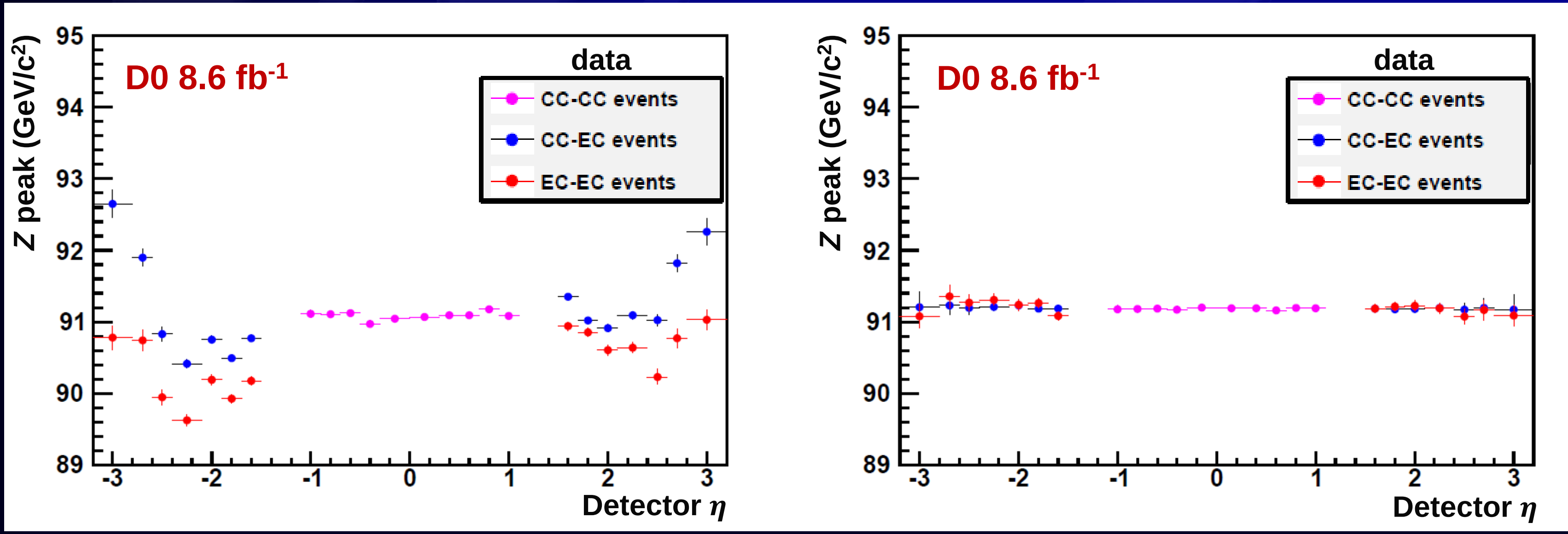

θ_W: $sin^2\theta_W$ Extraction

- **Raw A_{FB} measurement is compared to reweighted MC A_{FB} templates corresponding to different $sin^2\theta_W$ values**
  - Different $sin^2\theta_W$ predictions obtained by reweighting generator level 2D $(M_{Z/\gamma^*}, cos\theta^*)$ distribution of default MC ($sin^2\theta_W = 0.232$)
  - Done separately for CC-CC, CC-EC, EC-EC events, and for RunIIa (1.1 fb^{-1} low L_{inst}) and RunIIb (8.6 fb^{-1} high L_{inst}) running periods